



HAL
open science

Modeling Flow and Pressure Control in Water Distribution Systems Using the Nash Equilibrium

Jochen W Deuerlein, Sylvan Elhay, Olivier Piller, Angus R Simpson

► **To cite this version:**

Jochen W Deuerlein, Sylvan Elhay, Olivier Piller, Angus R Simpson. Modeling Flow and Pressure Control in Water Distribution Systems Using the Nash Equilibrium. *Journal of Water Resources Planning and Management*, 2023, 149 (6), pp.04023019. 10.1061/JWRMD5.WRENG-5889. hal-04054867

HAL Id: hal-04054867

<https://hal.inrae.fr/hal-04054867>

Submitted on 1 Apr 2023

HAL is a multi-disciplinary open access archive for the deposit and dissemination of scientific research documents, whether they are published or not. The documents may come from teaching and research institutions in France or abroad, or from public or private research centers.

L'archive ouverte pluridisciplinaire **HAL**, est destinée au dépôt et à la diffusion de documents scientifiques de niveau recherche, publiés ou non, émanant des établissements d'enseignement et de recherche français ou étrangers, des laboratoires publics ou privés.

Author-produced version of the article published in Journal of Water Resources Planning and Management, 149(6), 04023019. The original publication is available at <https://ascelibrary.org/doi/abs/10.1061/JWRMD5.WRENG-5889>.

- Jochen W. Deuerlein, Sylvan Elhay, Olivier Piller and Angus R. Simpson, Modeling Flow and Pressure Control in Water Distribution Systems Using the Nash Equilibrium, Journal of Water Resources Planning and Management 149 (2023), no. 6, 04023019.

Modelling Flow and Pressure Control in Water Distribution Systems Using the Nash Equilibrium

Jochen W. Deuerlein¹ Sylvan Elhay² Olivier Piller³

Angus R. Simpson, M.ASCE⁴

March 14, 2023

Abstract

Pressure dependent modelling (PDM) for water distribution systems (WDSs) is now widely accepted as being much more realistic than the previously used demand driven modelling (DDM). Steady-state linkflows, q , outflows, c , and heads, h , of a PDM WDS with no controls of flow and pressure in the system can reliably be found as the active set method (ASM) solution of a linear-equality-constrained nonlinear optimization of the system's content. Introducing linkflow controls, such as flow control valves (FCVs) and check valves (CVs) can be handled by imposing box constraints on the decision variables q and c in the optimization and these problems too can be found either by an ASM or an interior point method. The heads in these problems are the Lagrange multipliers in the content model and controlling these cannot be handled simply by imposing constraints on them. In this paper the problem of modelling pressure control devices such as pressure reducing valves (PRVs) is solved by finding the Nash Equilibrium of a model that treats (i) the (global) linkflow constrained content optimization and (ii) the local pressure controls, as players in a competitive, non-cooperative game. While this paper details how to model FCVs and PRVs together, this modelling framework is equally applicable to pressure sustaining valves and variable speed pumps for pressure control without essential modification.

¹Senior Researcher, 3S Consult GmbH, Albtalstrasse 13, D 76137 Karlsruhe, Germany & Adjunct Senior Lecturer, School of Civil, Environmental & Mining Engineering, University of Adelaide, South Australia, 5005.

²Visiting Research Fellow, School of Computer Science, University of Adelaide, South Australia, 5005, sylvan.elhay@adelaide.edu.au.

³Senior Research Scientist, INRAE, Dept. of Water, Bordeaux Regional Centre, UR ETTIS, 50 Ave. de Verdun, Gazinet, F-33612 Cestas, France & Adjunct Senior Lecturer, School of Civil, Environmental & Mining Engineering, University of Adelaide, South Australia, 5005.

⁴Professor, School of Civil, Environmental & Mining Engineering, University of Adelaide, South Australia, 5005.

An important contribution of this proof-of-concept paper is the development of a comprehensive model that includes flow and pressure controls and which finds a solution without using any heuristics. The new method is illustrated on some examples.

Keywords: Nash Equilibrium, pressure control, water distribution systems, steady-state pressure dependent modelling, active set methods, flow control valve, pressure reducing valve

INTRODUCTION

Pressure dependent modelling (PDM) for water distribution systems (WDSs) is now widely accepted as being much more realistic than the previously used demand driven modelling (DDM) (Cross 1936, Martin & Peters 1963, Wood & Charles 1972, Todini & Pilati 1988). Whereas DDM can produce mathematically correct solutions which are not realizable, PDM solutions take into account the change in delivery that actually occurs when nodal pressures are insufficient. PDM systems require a pressure outflow relationship (POR) which describes the outflow at each demand node as a function of available pressure: nodes at which the pressure head is below a preset minimum level, h_m , have zero outflow while those at which the available pressure is above a maximum preset service pressure head h_s , will have the nominal demand delivered. The POR describes the proportion of the nominal demand that is delivered for pressure heads between h_m and h_s .

Many different approaches to solving PDM problems have been seen in the literature (Bhave 1981, Tabesh 1998, Jun & Guoping 2013, Lippai & Wright 2014). These methods range from adding fictitious devices to emulate POR behaviour to repeatedly solving DDM problems and adjusting network demands to arrive at a steady state delivery. In fact, the steady-state linkflows, q , outflows, c , and heads, h , of a PDM WDS with no controls of flow and pressures in the system can reliably be found (Deuerlein et al. 2019) as the solution of a linear-equality-constrained nonlinear optimization of the system's content (Collins et al. 1978): the mass balance conditions impose the linear equality constraints and the heads are their Lagrange multipliers. Importantly, the Active Set Method (ASM) for this approach used the inverse POR function in the content. It is now well established that the methods which use the POR directly can require damping and other techniques to assist the iterative schemes with convergence while methods that use the inverse POR do not require special techniques and obtain PDM solutions in much the same time as direct methods take for DDM problems (Todini et al. 2022). Note that in a network that has no control valves or pumps the head loss is modelled by a monotone, non-decreasing function of the flow rate, $\Delta h = f(q)$. Fig. 1 (a) shows a typical head loss to flow relationship when there is no flow control. EPANET 2.2 (Rossman et al. 2020) has the capacity to solve PDM problems.

More detail on PDM methods can be found in Todini et al. (2022), Mahmoud et al. (2017),

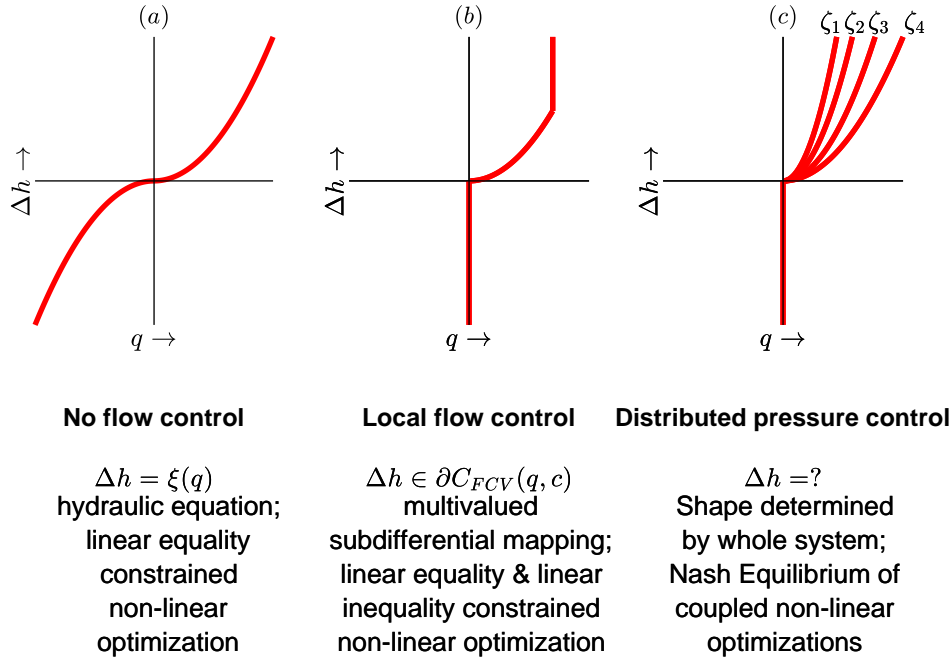


Figure 1: Comparison of the functional relationship between the flow and the head loss (i) in a link with no flow or pressure control, (ii) The multivalued subdifferential mapping of an FCV device content (Rockafellar 1970) and (iii) the content of a PRV device.

Deuerlein et al. (2019) and the references therein.

The design and management of modern WDSs requires the capacity to also model their control devices: pressure reducing valves (PRVs), flow control valves (FCVs), pressure sustaining valves (PSVs), check valves (CVs), throttle control valves (TCVs) and pumps. In general, control devices are used to enforce that the flows and pressures in the system are always within given operational limits. In addition, Abraham et al. (2018) propose a method that uses control valves to improve water quality by increasing flow velocity in the pipes. Piller & van Zyl (2014) used external quadratic penalty function terms added to a valve’s head loss equation to model FCVs. CVs were modelled, taking into account the direction of flow, as FCVs with a minimum flow setting of zero. Alvarruiz et al. (2015) modelled closed CVs as zero-flow pipes and FCVs as valves with flow at a preset level. Their scheme, which is based on the loop method, used the same heuristics as EPANET to determine device status and was applied only to DDM problems. In Alvarruiz et al. (2018) the authors improved on this work by using penalty methods (high resistance links). Gorev et al. (2018) treated FCVs, PRVs, PSVs as links with adjustable resistance and extended EPANET 2 to add artificial devices.

FCVs can be introduced into the model by adding linkflow constraints: the linkflows are required to lie between finite upper and lower limits. This problem too is a box constrained optimization which can, in most cases, be efficiently solved by an ASM technique (Piller et al.

2020). But the extra constraints can, for some networks, challenge an ASM. However, a method that is a hybrid between an ASM and an interior point method (IPM) (Elhay et al. 2021) has proved successful in solving even the difficult cases. Note that the constraints in both problems discussed so far are applied to the decision variables, q and c .

When flow controls are introduced into the problem, the relationship between the linkflow and the head loss takes the form of a multivalued mapping. Fig. 1 (b) shows this case when the flow is limited below by zero and above by a fixed upper limit seen by the vertical upper extension to the right of the curve. The control is applied as a local constraint on the linkflow.

Introducing pressure control devices such as PRVs or PSVs presents a more difficult problem because the pressure controls constrain the heads, which, as noted already, are the Lagrange multipliers in the content model. The approach taken in this paper is to introduce another decision variable, z , which represents the head reduction that is imposed by the PRV constraint which limits, if possible, the head at the node to be controlled to the desired setting value. The variable z is referred to here as the link's unknown local valve head loss and is defined in terms of the valve coefficient, ζ by $z = \zeta q|q|/(2gA^2)$, A the pipe area.

Foglianti et al. (2020) introduce two methods for modelling a WDS with pressure control. The first imposes the set head on the node with pressure controlled by an active PRV and adds a new unknown which represents the head loss due to the active valve and then adjusts the model to account for this. The resulting model has an unsymmetric linear system. The second method also imposes a set pressure on the node being controlled but removes the pipe with the valve and modifies the mass balance equations at the node at the other end of the PRV link. This approach leads to a symmetric linear system. Wu et al. (2009) propose an extended solution method which calculates the pump speed required to achieve the desired hydraulic heads or fixed pump flows. Estrada et al. (2009) reports the “results of the research on computational strategies capable of dealing with low resistance elements, hydrant modelling, multiple regulation valves, numerous emitters, and pumps with complex curves” and write that their GESTAR software can achieve rapid convergence even where other software fails to converge. One disadvantage of previously developed methods is that they require heuristics which depend on interrogating the valve states at each iteration.

The novel technique described in this paper extends work on the use of Game Theory and the Nash Equilibrium (Deuerlein 2002, Deuerlein et al. 2005) to PDM WDSs with flow and pressure controls. Its framework includes a comprehensive mathematical model of the system which provides a solution with uniquely determined valve states. Basing the solution on the Karush-Kuhn-Tucker (KKT) conditions for the players in the game (the control devices [PRVs, PSVs, pumps] on the one hand and the system's content on the other) leads to finding the Lagrange multipliers which represent a part of the solution. As well, degenerate operational conditions

for PRVs and FCVs which lead to singular systems and the consequent non-uniqueness of solutions are clearly explained by the method and lead to recommendations for the prevention of unstable system behaviour in real systems.

The rest of the paper is organized as follows. The next section introduces some definitions and notation. The section after that introduces the Nash Equilibrium and illustrates its use on two simple examples. The next section formally states the problem addressed in this paper and describes the new method of solution. The sections following discuss some implementation issues and present some illustrative examples of the method. The last section presents some conclusions and suggestions for future work.

DEFINITIONS AND NOTATION

Consider a WDS whose network graph has n_p links, or arcs, and $n_j + n_f$ nodes, or vertices: n_j is the number of nodes at which the heads are unknown and $n_f \geq 1$ is the number of source or sink nodes with fixed heads. The links of the network include control valves, pumps and pipes. Denote by $\mathbf{q} = (q_1, q_2, \dots, q_{n_p})^T \in \mathbb{R}^{n_p}$ the vector of unknown flows in the system, $\mathbf{h} = (h_1, h_2, \dots, h_{n_j})^T \in \mathbb{R}^{n_j}$ the unknown heads at the nodes in the system, $\mathbf{u} = (u_1, u_2, \dots, u_{n_j})^T \in \mathbb{R}^{n_j}$ the vector of node ground elevations and $\mathbf{r}(\mathbf{q}) = (r_1, r_2, \dots, r_{n_p})^T$ the vector of link resistance factors. Let \mathbf{A} denote the $n_p \times n_j$, full rank, unknown-head Arc-Node Incidence Matrix (ANIM): the ji element of \mathbf{A} is (i) -1 if node i is at the end of arc j , (ii) 0 if arc j does not connect to the node i , and (iii) 1 if arc j starts at node i . Let \mathbf{A}_0 denote the ANIM, with a similar definition, for the fixed-head nodes. Let \mathbf{h}^0 denote the vector of heads of the n_f fixed-head nodes. Denote $\mathbf{a} = \mathbf{A}_0 \mathbf{h}^0$. Denote by η the exponent used in the head loss formula: $\eta = 2$ for the Darcy-Weisbach model and $\eta = 1.852$ for the Hazen-Williams model. Furthermore, denote by $\mathbf{G}(\mathbf{q}) \in \mathbb{R}^{n_p \times n_p}$ the diagonal matrix whose diagonal elements are defined as $[\mathbf{G}(\mathbf{q})]_{jj} = r_j |q_j|^{\eta-1}$. Then, $\boldsymbol{\xi}(\mathbf{q}) = (\xi_1(q_1), \xi_2(q_2), \dots, \xi_{n_p}(q_{n_p}))^T = \mathbf{G}(\mathbf{q})\mathbf{q}$ is the vector whose elements model the frictional head losses of the pipes in the system. In general, (e.g. for the Darcy-Weisbach formula) $\mathbf{r} = \mathbf{r}(\mathbf{q})$ but for the Hazen-Williams formula \mathbf{r} is independent of \mathbf{q} . Denote the vector of the nominal demands at the nodes with unknown-head by $\mathbf{d} = (d_1, d_2, \dots, d_{n_j})^T \in \mathbb{R}^{n_j}$ and denote by n_d the number of nodes with non-zero demands. Denote by $\mathbf{c}(\mathbf{h}, \mathbf{d}) \in \mathbb{R}^{n_j}$ the vector whose elements are the POR function values at the n_j nodes of the system and denote $\mathbf{1} = (1, 1, \dots, 1)^T$. Denote by n_v the number of PRVs in a network and by ζ the valve coefficient. Rather than ζ , the local valve head loss variable defined as $z = \zeta |q| q$ will be used. Denote by $\mathbf{z} = (z_1, z_2, \dots, z_{n_v})^T$, the local valve head losses resulting from the PRVs in the system. The notation $f(a: x, y)$ indicates that f is a function of the independent variables x, y and the parameter a .

Throughout what follows, the symbol \mathbf{O} denotes a zero matrix and \mathbf{o} denotes a zero column

vector of appropriate dimension for the particular case. The shorthand notation $\mathbf{x} + a$, where \mathbf{x} is a vector and a is a scalar, will be used to denote the case where every component of \mathbf{x} has a added to it. Furthermore, it will be assumed that any matrix inverses which are shown, do in fact, exist. The following Matlab-like notation (Matlab 2020a) will be used: $\mathbf{X}(s, :)$ will denote a submatrix of the matrix \mathbf{X} made up of the rows indexed by the set s and all columns.

Denote by $\mathbf{S}_s \in \mathbb{R}^{n_v \times n_j}$ the selection matrix for those nodes at the start of a PRV link, $\mathbf{S}_e \in \mathbb{R}^{n_v \times n_j}$ the selection matrix for those nodes at the end of a PRV link (i.e. which have a set pressure head) and $\mathbf{L}_{n_v} \in \mathbb{R}^{n_v \times n_p}$ the selection matrix for those links which have a PRV. Let $\mathbf{L}_{z_a} \in \mathbb{R}^{n_{z_a} \times n_v}$ denote the matrix which selects only those components of \mathbf{z} which are zero (i.e. those z for which the z -constraint $z \geq 0$ is saturated). Denote by N_v the set of indices of the links which have PRVs.

Turning now to PDM problems, assume, for simplicity and without loss of generality, that every demand node has the same minimum pressure head, h_m , and the same service pressure head, h_s . Individualized minimum and service pressure heads can be implemented by replacing h_m by h_{mi} and h_s by h_{si} throughout but presents no further difficulty. This modification does not change the method and only complicates data management and notation.

Define the head fraction, in terms of the nodal head (elevation head plus pressure head), h , by

$$\omega(h) \stackrel{\text{def}}{=} (h - (u + h_m)) / (h_s - h_m).$$

Suppose that $\gamma(\cdot)$ is a bounded, smooth, monotonically increasing function which maps the interval $[0, 1] \rightarrow [0, 1]$. The POR at a node is defined by

$$c(h_i) = \begin{cases} 0 & \text{if } \omega(h_i) \leq 0 \\ d_i \gamma(\omega(h_i)) & \text{if } 0 < \omega(h_i) < 1. \\ d_i & \text{if } \omega(h_i) \geq 1 \end{cases} \quad (1)$$

The inverse function of the POR, the head, $h_i(c)$ expressed as a function of outflow c_i at node i , will be required for the development of the new method. But, the function $h(c_i)$ is not in general everywhere differentiable and so in its place a multivalued, sub-differential mapping is considered for those nodes at which $d_i > 0$:

$$h(c_i) = \begin{cases} \emptyset & \text{if } c_i < 0 \\ (-\infty, u_i + h_m] & \text{if } c_i = 0 \\ (h_s - h_m) \gamma^{-1} \left(\frac{c_i}{d_i} \right) + u_i + h_m & \text{if } 0 < c_i < d_i. \\ [u_i + h_s, +\infty) & \text{if } c_i = d_i \\ \emptyset & \text{if } c_i > d_i \end{cases} \quad (2)$$

A discussion of several common PORs, their derivatives, their inverses and their derivatives

can be found in [Deuerlein et al. \(2019\)](#). Note that, in what follows, careful distinction is made between the scalar variables, h , which represent the heads and the multivalued, sub-differential mapping function, $h(\cdot)$, which represents the inverse POR.

Certain of the links in the networks under consideration will have FCVs. For these links the flow will be restricted to lie between a fixed and finite lower bound and a fixed and finite upper bound: $q_{k,min} \leq q_k \leq q_{k,max}$. As a formalism the flows in all links in the network are constrained to lie between a lower and an upper bound but a bound is set to $\pm\infty$ if it is not finite.

In the present model, to which we shall refer as the Nash Equilibrium for pressure control (NEPC), when a PRV is required, it is introduced adjacent to the downstream node of a network link and this PRV determines the local valve head loss using only local information: the link's flow, it's frictional head loss, the upstream node's head and the downstream node's set pressure head. In more detail, if, in the present model, the link k , in which the direction of flow is from node i_k to node j_k , has a PRV, that will be taken to mean that the PRV is adjacent to node, j_k , and is attempting to ensure that the head at node j_k never exceeds a (predetermined) value, $h_{j_k}^s$ (the elevation head plus set pressure head for the PRV). It is worth repeating that, unlike many of the other pressure control models in the literature (e.g. EPANET), here there is a frictional head loss, $\xi(q_k)$, associated with a link which has a PRV. This consequence of the implementation, however, imposes no limitations on the method. The flows in PRV links are constrained to be non-negative: $0 \leq q_k \leq \infty$. In addition, it is assumed that (i) no link can have both an FCV and PRV, (ii) all PRV nodes have zero demands to avoid a violation of the Linear Inequality Constraint Qualification (LICQ) because a POR constraint and a z -constraint saturate simultaneously and (iii) there is always a path made up of links with unsaturated flow constraints between the PRV link's upstream node and a source. If assumption (iii) is violated, a PRV link node could become isolated, leading to an ill-posed problem ([Piller et al. 2022](#)).

In common engineering terminology, a PRV can assume the states of **open** (**inactive**), **active** or **closed**. These states are defined by combinations, shown in Table 1, of the variables q , κ , z and χ . The following terminology will be used here in the interests of clarity: in what follows a z -constraint, $z \geq 0$, will be imposed on the PRV link local valve head loss and the constraint will be said to be **saturated** (rather than **active**) when $z = 0$ to avoid confusion of the valve's status with the constraint's status.

THE NASH EQUILIBRIUM

The linkflows, outflows and heads of the problem are found here, as before, from the optimization, by an ASM, of the system's content but taking into account the local valve head losses. However, before describing more detail of the problem and its solution the Nash Equilibrium

Status	z	χ	κ	q	Relation
Open	0	> 0	0	> 0	$h_{i_k} > h_{j_k}, h_{j_k}^s > h_{j_k}$
Active	> 0	0	0	> 0	$h_{i_k} > h_{j_k}^s = h_{j_k}$
Closed 1	> 0	0	> 0	0	$h_{i_k} > h_{j_k} > h_{j_k}^s$
Closed 2	> 0	0	> 0	0	$h_{j_k} > h_{i_k} > h_{j_k}^s$
Closed 3	0	> 0	> 0	0	$h_{j_k} > h_{j_k}^s > h_{i_k}$

Table 1: Table showing the relations between PRV status and some link and node parameters

is introduced.

Consider a continuous, non-cooperative game between two players. The response of each player to moves by their opponent can be described by a function. The functions which characterise the best responses by the two players are known as the *best reply* functions. If these two functions intersect, the point at which they intersect characterises the Nash Equilibrium: the point at which neither player has anything to gain by changing their strategy. Readers interested in game theory and Cournot-Nash Equilibrium are referred to [Osborne & Rubinstein \(1994\)](#) or [Bonanno \(2018\)](#) or [Friedman \(1986\)](#).

To illustrate the Nash Equilibrium with a simple example related to WDSs consider the network shown in Fig. 2. It has a PRV at the downstream end of link 1 which is intended to control the head at node 2. Nodes 3 and 4 have fixed heads: $h_3^0 = 60$ m and $h_4^0 = 30$ m. Nodes 1 and 2 have elevations $u_1 = u_2 = 0$ m. All links have length 400 m and they all have diameters 500 mm and pipe roughnesses 0.25 mm. The head losses are modelled by the Darcy-Weisbach formulae and there is a prescribed head set point, h^s , for the head at node 2. The two nodes with unknown head have zero demands.

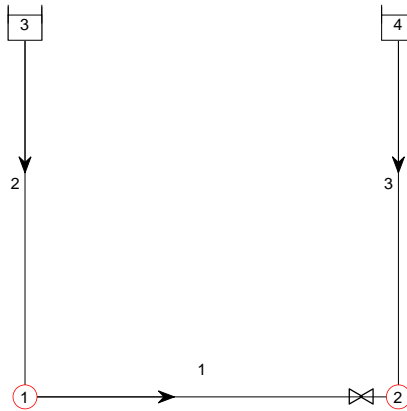


Figure 2: The network with one PRV used to generate the best reply functions shown in Fig. 3

An analysis of this network using the new modelling framework of this paper can be found in Appendix B. Mass balance for the system requires $q_1 = q_2 = -q_3 \stackrel{\text{def}}{=} q$ and the resistance factors satisfy $r_1 = r_2 = r_3 \stackrel{\text{def}}{=} r$. The best reply function for the flows is found from the function

$$q(z) = +\sqrt{\frac{|h_3^0 - h_4^0 - z|}{3r}} \quad (3)$$

in which the flow is expressed as function of the local valve head loss. Note that for the Hazen-Williams head loss model r is independent of q but for the Darcy-Weisbach head loss, $r = r(q)$ and $q(z)$ is defined implicitly by Eq. (3). In turn, the best reply function for the local valve head loss is

$$z(q) = h_3^0 - 2r|q|q - h^s \quad (4)$$

where z is expressed as a function of q . Fig. 3 shows this network's best reply functions for four different head set points $h^s = 28, 31, 35$ and 50 m. Note that, since the elevations are all zero, these are also the set pressure heads for the PRV. In each case the Nash Equilibrium is shown by a dot (\bullet). The case $h^s = 28$ m shows κ , the Lagrange multiplier for the lower bound linkflow constraint as the difference between $z(0)$ and the value of z at which $q(z) = 0$. For $h^s = 31$ m and $h^s = 35$ m the Nash Equilibrium point is in the interior of the region (the point where the two curves intersect) and for the last case, $h^s = 50$ m, the Nash Equilibrium point is where the extension of the $z(q)$ curve along the horizontal axis intersects with $q(z)$.

Consider the network shown in Fig. 4 in which there are two control valves in series, C_1 and C_2 , each of which can be either an FCV or a PRV. The FCV limits the flow in its link to $q_{max} = 300$ L/s in all three cases.

Fig. 5 shows three examples illustrating the Nash Equilibrium for this network. Fig. 5 (a) shows the case where $C_1 = \text{FCV}$ and $C_2 = \text{PRV}$. The FCV constraint is saturated (the valve's status is active) and the PRV constraint is saturated (the PRV is fully open, $z = 0$) so the PRV plays no role. The Nash Equilibrium point is shown by a dot at the intersection of the extension of the $q(z)$ curve where the flow is restricted by the FCV (the vertical red line) and the x-axis. The intersection of the $q(z)$ and $z(q)$ curves lies outside the feasible flow set showing that the FCV constraint is more restrictive than the PRV constraint. Both devices can't be in an active control state since this violates the assumption that there is always a path with unsaturated links between a source and the PRV.

Fig. 5 (b) shows the case where $C_1 = \text{PRV}$ and $C_2 = \text{FCV}$. Here the FCV constraint is saturated (the valve's status is active) and the PRV is in active mode (its constraint is unsaturated, $z > 0$). The Lagrange multiplier for the upper flow bound, ν^* , is shown as the vertical distance between the Nash Equilibrium point and the point where the flow $q(z)$ is limited to 300 L/s.

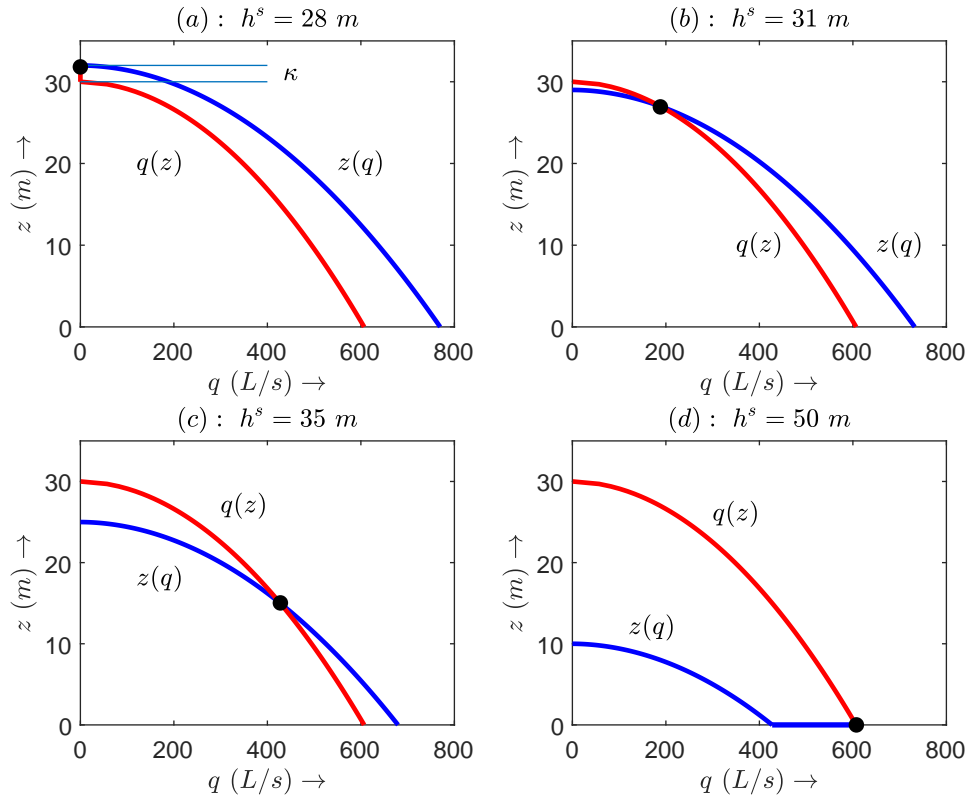


Figure 3: The best reply functions indicating the Nash Equilibrium (●) for the network shown in Fig. 2. Flow, $q(z)$, is measured in L/s and local valve head loss, $z(q)$, is measured in m .

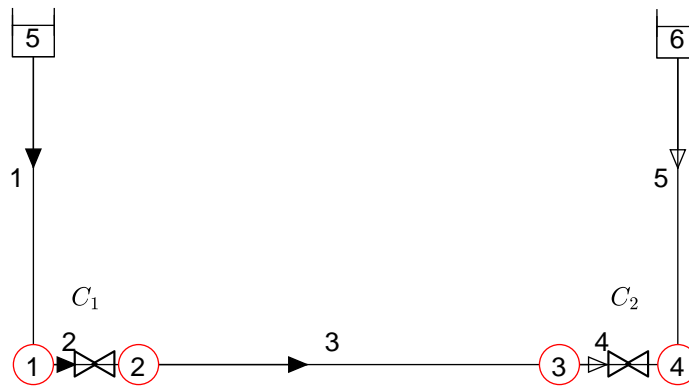


Figure 4: A model of the network used in Piller & van Zyl (2014) which has two controls, C_1 and C_2 , in series. The controls can be an FCV followed by a PRV or vice versa.

Fig. 5 (c) shows the case where $C_1 = \text{FCV}$ and $C_2 = \text{PRV}$ and where the point of intersection between $q(z)$ and $z(q)$ is the point where $q(z)$ meets the FCV upper bound limit. This problem has no unique solution and parallels the situation where the Linear Inequality Constraint Qualification (LICQ) condition is violated: any combination of ν^* and z^* such that $\nu^* + z^* = \omega^*$ gives a Nash Equilibrium at the point where z^* meets ν^* .

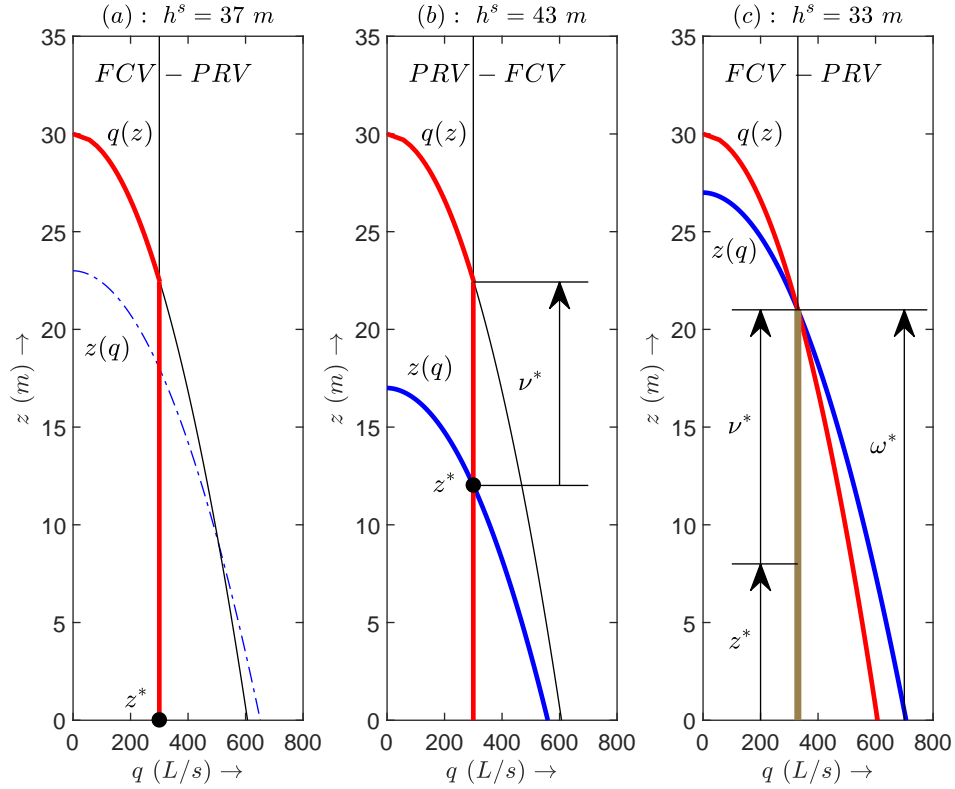


Figure 5: Examples of the Nash Equilibrium with two controls in series (a) FCV-PRV; the FCV constraint is saturated and the PRV is open (b) PRV-FCV; both control constraints are saturated and (c) FCV-PRV; the assumption that there is a path connecting every PRV link to a source such that no link in that path has a saturated flow constraint is violated. In all cases $q_{max} = 300$ L/s.

THE PROBLEM AND ITS SOLUTION BY OPTIMIZATION

More precisely, the problem addressed in this paper is:

Problem 1 *Given a PDM of a WDS network which has both FCVs and PRVs, find the system's steady-state linkflows, \mathbf{q} , nodal heads, \mathbf{h} , nodal outflows, \mathbf{c} , and PRV link local valve head losses, \mathbf{z} .*

The solution to Problem 1 is the Nash Equilibrium for a game in which the players are

- (a) the optimization of a system content model which incorporates the local valve head losses for each link with a PRV as fixed parameters, and
- (b) a separate, local optimization problem for each link with a PRV treating the linkflows and outflows and heads as fixed parameters.

If there are n_v PRVs in a system, these $n_v + 1$ optimization problems can be thought of as players competing in a non-cooperative game against each other. In this case there is no simple functional description or multivalued mapping such as in Fig. 1 (a) and (b) for the relationship between the head at a PRV node and the link's flow because the factors that determine the control of the head are distributed throughout the system. Fig. 1 (c) shows this situation for different fixed values of the valve loss coefficient, ζ . The final, or steady-state, value of ζ is determined by the additional condition that the pressure head is achieved at the PRV node. For illustration and to simplify the exposition, the problem will be said, in some instances, to be a game between two players: all the local optimization problems will be treated as one player, even though this is, strictly speaking, not so.

Treating the solution of Problem 1 as a Nash Equilibrium point means finding the solution of a differentiable, non-cooperative game. One player finds the linkflows, heads and outflows while treating the local valve head losses as a parameter, while the other players find the PRV link local valve head losses while treating the linkflows, outflows and head losses of the other PRVs as parameters. The game is now described in detail.

Player 1: Finding the Linkflows, Outflows and Heads

In this section the local valve head loss \mathbf{z} is considered as a fixed parameter and the decision variables are \mathbf{q} and \mathbf{c} . Taking the content function defined in Piller et al. (2020) and adding the term $\mathbf{z}^T \mathbf{q}$ to account for the fixed local valve head losses in PRV links gives the objective function, restricted to $\mathbf{o} \leq \mathbf{c} \leq \mathbf{d}$ and $\mathbf{q}_{min} \leq \mathbf{q} \leq \mathbf{q}_{max}$, in the Player 1 optimization:

$$C(\mathbf{z}; \mathbf{q}, \mathbf{c}) = \sum_{j=1}^{n_p} \int_0^{q_j} \xi_j(s) ds - \mathbf{a}^T \mathbf{q} + \mathbf{c}^T (\mathbf{u} + h_m) + \sum_{\substack{1 \leq i \leq n_j \\ d_i > 0}} (h_s - h_m) \int_0^{c_i} \gamma^{-1} \left(\frac{s}{d_i} \right) ds + \mathbf{z}^T \mathbf{q}. \quad (5)$$

Denote

$$\psi(c_i) = \begin{cases} (h_s - h_m) \int_0^{c_i} \gamma^{-1} \left(\frac{x}{d_i} \right) dx, & \text{if } d_i > 0 \\ 0 & \text{if } d_i = 0 \end{cases}$$

$$\boldsymbol{\psi}(\mathbf{c}) = (\psi(c_1), \psi(c_2), \dots, \psi(c_{n_j}))^T,$$

and let $\boldsymbol{\theta}(\mathbf{c})$ denote the scaled vector of inverse POR functions

$$\boldsymbol{\theta}(\mathbf{c}) = \nabla_{\mathbf{c}} \boldsymbol{\psi}(\mathbf{c}) = (h_s - h_m) (\gamma^{-1}(c_1/d_1), \gamma^{-1}(c_2/d_2), \dots, \gamma^{-1}(c_{n_j}/d_{n_j}))^T$$

Denote also $\mathbf{h}(\mathbf{c}) = \boldsymbol{\theta}(\mathbf{c}) + \mathbf{u} + h_m$.

The Lagrangian associated with this minimization problem is

$$\begin{aligned}
L_1(\mathbf{z}; \mathbf{q}, \mathbf{c}, \mathbf{h}, \boldsymbol{\lambda}^*, \boldsymbol{\mu}^*, \boldsymbol{\kappa}^*, \boldsymbol{\nu}^*) &= \sum_{j=1}^{n_p} \int_0^{q_j} \xi_j(s) ds - \mathbf{a}^T \mathbf{q} + \mathbf{1}^T \boldsymbol{\psi}(\mathbf{c}) + \mathbf{c}^T (\mathbf{u} + h_m) + \\
&\quad \mathbf{z}^T \mathbf{q} - \mathbf{h}^T (\mathbf{A}^T \mathbf{q} + \mathbf{c}) + \boldsymbol{\mu}^{*T} (\mathbf{c} - \mathbf{d}) - \boldsymbol{\lambda}^{*T} \mathbf{c} + \\
&\quad \boldsymbol{\kappa}^{*T} (-\mathbf{q} + \mathbf{q}_{min}) + \boldsymbol{\nu}^{*T} (\mathbf{q} - \mathbf{q}_{max}) \\
&\text{subject to } \boldsymbol{\lambda}^* \geq \mathbf{o}, \quad \boldsymbol{\mu}^* \geq \mathbf{o}, \quad \boldsymbol{\kappa}^* \geq \mathbf{o}, \quad \boldsymbol{\nu}^* \geq \mathbf{o}
\end{aligned}$$

with $\boldsymbol{\lambda}$ and $\boldsymbol{\mu}$ the Lagrange multipliers for the outflow constraints, $\boldsymbol{\kappa}$ and $\boldsymbol{\nu}$ the Lagrange multipliers for the flow constraints.

Player 2: Finding the PRV Local Valve Head Losses

In this section the primal variables, \mathbf{q} , \mathbf{c} , and \mathbf{h} , are considered fixed parameters and \mathbf{z} is considered a decision variable. There is one additional objective function

$$f(z_k) = \frac{1}{2} (h_{i_k} - \xi(q_k) - z_k - h_{j_k}^s)^2 \quad (6)$$

for each link, k , with a PRV in which the flow is from node i_k to node j_k , where the set nodal head is $h_{j_k}^s$ (elevation head plus set pressure head for the PRV). The minimization of these objective functions will be referred to as local minimization problems. The primal problem for local control is

$$\min_{z_k \geq 0} f(z_k) = \min_{z_k \geq 0} \frac{1}{2} (h_{i_k} - \xi(q_k) - z_k - h_{j_k}^s)^2 \quad (7)$$

and its associated saddle point problem is

$$\min_{z_k} \max_{\chi_k \geq 0} L_2(z_k, \chi_k) = \min_{z_k} \max_{\chi_k \geq 0} f(z_k) - \chi_k z_k \quad (8)$$

The Karush-Kuhn-Tucker (KKT) conditions necessary for optimality of the saddle point problem are

$$(a) \quad \frac{\partial L_2(z_k, \chi_k)}{\partial z_k} = - (h_{i_k} - \xi(q_k) - z_k - h_{j_k}^s) - \chi_k = 0 \quad (9)$$

$$(b) \quad \exists \tau \geq 0 \left| \frac{\partial (-L_2(z_k, \chi_k))}{\partial \chi_k} - \tau = z_k - \tau = 0 \right. \quad (10)$$

with $\tau \chi_k = 0$. At optimality we have $z_k \geq 0$ and $\chi_k z_k = 0$.

It is important to note again that there is one additional optimization problem (7) for *each*

link which has a PRV. Strictly speaking, each of these sub-problems represents another player in the game but for convenience they are referred to collectively when there is no ambiguity. Denote $\boldsymbol{\chi} = (\chi_1, \chi_2, \dots, \chi_{n_v})^T$. All the local minimization problem KKT conditions (9) and (10) can be collected into vector form:

$$\mathbf{S}_s \mathbf{h} - \mathbf{L}_{n_v} \boldsymbol{\xi}(\mathbf{q}) - \mathbf{z} + \boldsymbol{\chi} - \mathbf{h}^s = \mathbf{o} \text{ and } \mathbf{L}_{z_a} \mathbf{z} = \mathbf{o}. \quad (11)$$

The Combined Optimization

The Nash Equilibrium is the point which jointly solves the two optimization problems

$$\min_{\mathbf{q}, \mathbf{c}} C(\mathbf{z}; \mathbf{q}, \mathbf{c}) \quad (12)$$

$$\text{subject to} \quad (13)$$

$$-\mathbf{A}^T \mathbf{q} - \mathbf{c} = \mathbf{o}, \quad (14)$$

$$-\mathbf{c} \leq \mathbf{o}, \quad (15)$$

$$\mathbf{c} \leq \mathbf{d}, \quad (16)$$

$$\mathbf{q} - \mathbf{q}_{max} \leq \mathbf{0}, \quad (17)$$

$$-\mathbf{q} + \mathbf{q}_{min} \leq \mathbf{0}, \quad (18)$$

and

$$\min_{z_k} \frac{1}{2} (h_{i_k} - \xi(q_k) - z_k - h_{j_k}^s)^2, \quad k \in N_v \quad (19)$$

$$\text{subject to} \quad (20)$$

$$-z_k \leq 0, \quad (21)$$

Here, as later, some subscripts have been omitted to clarify the exposition when there is no ambiguity.

Figures C.1–C.5 of Appendix C show examples of the node and link parameters for PRVs which are open, active or closed. In particular, Figs. C.3–C.5, show how it is possible for the local valve head loss, z , to take on zero and positive values when the valve status is closed ($q_k = 0$).

The corresponding valve links can have $q \geq 0$ and their device status can be either **closed** or **open** and they will be allocated to an index set denoted by \mathcal{I}_{z_a} . By comparison, PRV links for which $z > 0$ have unsaturated z -constraints, they have $q \geq 0$ and their device status can be either **closed** or **active**. They will be allocated to an index set denoted by \mathcal{I}_{z_b} .

The Nash Equilibrium is the point at which the various best reply functions for the competing players intersect and so it can be found, in view of the problem's convexity, as the point

which satisfies the necessary and sufficient KKT conditions for (12) – (21). That is to say (i) the KKT conditions that follow from zeroing the gradient of the Lagrangian for Player 1 and (ii) the $n_v + \cdot$ KKT conditions which are encapsulated in (11):

$$\boldsymbol{\xi}(\mathbf{q}) - \mathbf{A}\mathbf{h} - \mathbf{a} - \mathbf{L}_q^T \boldsymbol{\kappa} + \mathbf{U}_q^T \boldsymbol{\nu} + \mathbf{L}_{n_v}^T \mathbf{z} = \mathbf{o} \in \mathbb{R}^{n_p} \quad (22)$$

$$\mathbf{h}(\mathbf{c}) - \mathbf{h} - \mathbf{L}_c^T \boldsymbol{\lambda} + \mathbf{U}_c^T \boldsymbol{\mu} = \mathbf{o} \in \mathbb{R}^{n_j} \quad (23)$$

$$-\mathbf{A}^T \mathbf{q} - \mathbf{c} = \mathbf{o} \in \mathbb{R}^{n_j} \quad (24)$$

$$-\mathbf{L}_c \mathbf{c} = \mathbf{o} \in \mathbb{R}^{n_{c_l}} \quad (25)$$

$$\mathbf{U}_c(\mathbf{c} - \mathbf{d}) = \mathbf{o} \in \mathbb{R}^{n_{c_u}} \quad (26)$$

$$-\mathbf{L}_q(\mathbf{q} - \mathbf{q}_{min}) = \mathbf{o} \in \mathbb{R}^{n_{q_l}} \quad (27)$$

$$\mathbf{U}_q(\mathbf{q} - \mathbf{q}_{max}) = \mathbf{o} \in \mathbb{R}^{n_{q_u}} \quad (28)$$

$$\mathbf{S}_s \mathbf{h} - \mathbf{L}_{n_v} \boldsymbol{\xi}(\mathbf{q}) - \mathbf{z} + \mathbf{L}_{z_a}^T \boldsymbol{\chi}_{z_a} - \mathbf{h}^s = \mathbf{o} \in \mathbb{R}^{n_v} \quad (29)$$

$$\mathbf{L}_{z_a} \mathbf{z} = \mathbf{o} \in \mathbb{R}^{n_{z_a}} \quad (30)$$

$$-\mathbf{c} \leq \mathbf{o} \in \mathbb{R}^{n_j} \quad (31)$$

$$\mathbf{c} - \mathbf{d} \leq \mathbf{o} \in \mathbb{R}^{n_j} \quad (32)$$

$$-\mathbf{q} - \mathbf{q}_{min} \leq \mathbf{o} \in \mathbb{R}^{n_p} \quad (33)$$

$$\mathbf{q} - \mathbf{q}_{max} \leq \mathbf{o} \in \mathbb{R}^{n_p} \quad (34)$$

$$-\mathbf{z} \leq \mathbf{o} \in \mathbb{R}^{n_v} \quad (35)$$

$$\boldsymbol{\lambda} \geq \mathbf{o}, \quad \boldsymbol{\mu} \geq \mathbf{o}, \quad \boldsymbol{\kappa} \geq \mathbf{o}, \quad \boldsymbol{\nu} \geq \mathbf{o}, \quad \boldsymbol{\chi} \geq \mathbf{o} \quad (36)$$

Here

- (a) \mathbf{L}_\bullet is a matrix made up of rows of the identity whose indices correspond to those of the nodes (subscript c) or links (subscript q) or PRV local valve head losses (subscript z) at which the lower (POR, linkflow or local valve head loss) constraint is saturated (or binding).
- (b) \mathbf{U}_\bullet is a matrix made up of rows of the identity whose indices correspond to those of the nodes (subscript c) or links (subscript q) at which the upper (POR or linkflow) constraint is saturated.

This system is solved with an ASM (Hager & Zhang 2006). The Jacobian of (22)–(35) is

$$\begin{array}{c}
 n_p \\
 n_j \\
 n_j \\
 n_{c_l} \\
 n_{c_u} \\
 n_{q_l} \\
 n_{q_u} \\
 n_v \\
 n_{z_a}
 \end{array}
 \begin{pmatrix}
 n_p & n_j & n_j & n_{c_l} & n_{c_u} & n_{q_l} & n_{q_u} & n_v & n_{z_a} \\
 \mathbf{F}(\mathbf{q}) & \mathbf{O} & -\mathbf{A} & \mathbf{O} & \mathbf{O} & -\mathbf{L}_q^T & \mathbf{U}_q^T & \mathbf{L}_{n_v}^T & \mathbf{O} \\
 \mathbf{O} & \mathbf{M}(\mathbf{c}) & -\mathbf{I} & -\mathbf{L}_c^T & \mathbf{U}_c^T & \mathbf{O} & \mathbf{O} & \mathbf{O} & \mathbf{O} \\
 -\mathbf{A}^T & -\mathbf{I} & \mathbf{O} \\
 \mathbf{O} & -\mathbf{L}_c & \mathbf{O} \\
 \mathbf{O} & \mathbf{U}_c & \mathbf{O} \\
 -\mathbf{L}_q & \mathbf{O} \\
 \mathbf{U}_q & \mathbf{O} \\
 -\mathbf{L}_{n_v} \mathbf{F}(\mathbf{q}) & \mathbf{O} & \mathbf{S}_s & \mathbf{O} & \mathbf{O} & \mathbf{O} & \mathbf{O} & -\mathbf{I}_{n_v} & \mathbf{L}_{z_a}^T \\
 \mathbf{O} & \mathbf{L}_{z_a} & \mathbf{O}
 \end{pmatrix}. \quad (37)$$

where $\mathbf{M}(\mathbf{c}) \in \mathbb{R}^{n_j \times n_j}$ is the diagonal matrix of the derivatives of the inverse function, $\mathbf{h}(\mathbf{c})$. Unlike its counterpart in Piller et al. (2020), this matrix is not symmetric. This fact is briefly discussed later. The Newton method for the system is

$$\begin{pmatrix}
 \mathbf{F}^{(m)} & \mathbf{O} & -\mathbf{A} & \mathbf{O} & \mathbf{O} & -\mathbf{L}_q^{(m)T} & \mathbf{U}_q^{(m)T} & \mathbf{L}_{n_v}^T & \mathbf{O} \\
 \mathbf{O} & \mathbf{M}^{(m)} & -\mathbf{I} & -\mathbf{L}_c^{(m)T} & \mathbf{U}_c^{(m)T} & \mathbf{O} & \mathbf{O} & \mathbf{O} & \mathbf{O} \\
 -\mathbf{A}^T & -\mathbf{I} & \mathbf{O} \\
 \hline
 \mathbf{O} & -\mathbf{L}_c^{(m)} & \mathbf{O} \\
 \mathbf{O} & \mathbf{U}_c^{(m)} & \mathbf{O} \\
 -\mathbf{L}_q^{(m)} & \mathbf{O} \\
 \mathbf{U}_q^{(m)} & \mathbf{O} \\
 \hline
 -\mathbf{L}_{n_v} \mathbf{F}^{(m)} & \mathbf{O} & \mathbf{S}_s & \mathbf{O} & \mathbf{O} & \mathbf{O} & \mathbf{O} & -\mathbf{I}_{n_v} & \mathbf{L}_{z_a}^{(m)T} \\
 \mathbf{O} & \mathbf{L}_{z_a}^{(m)} & \mathbf{O}
 \end{pmatrix} \times \quad (38)$$

$$\begin{aligned}
& \begin{pmatrix} \delta \mathbf{q}^{(m+1)} \\ \delta \mathbf{c}^{(m+1)} \\ \delta \mathbf{h}^{(m+1)} \\ \hline \delta \boldsymbol{\lambda}^{(m+1)} \\ \delta \boldsymbol{\mu}^{(m+1)} \\ \delta \boldsymbol{\kappa}^{(m+1)} \\ \hline \delta \boldsymbol{\nu}^{(m+1)} \\ \hline \delta \mathbf{z}^{(m+1)} \\ \delta \boldsymbol{\chi}_{z_a}^{(m+1)} \end{pmatrix} \\
= & - \begin{pmatrix} \mathbf{G}(\mathbf{q}^{(m)})\mathbf{q}^{(m)} - \mathbf{A}\mathbf{h}^{(m)} - \mathbf{a} - \mathbf{L}_q^{(m)T} \boldsymbol{\kappa}^{(m)} + \mathbf{U}_q^{(m)T} \boldsymbol{\nu}^{(m)} + \mathbf{L}_{n_v}^T \mathbf{z}^{(m)} \\ \mathbf{h}(\mathbf{c}^{(m)}) - \mathbf{h}^{(m)} - \mathbf{L}_c^{(m)T} \boldsymbol{\lambda}^{(m)} + \mathbf{U}_c^{(m)T} \boldsymbol{\mu}^{(m)} \\ -\mathbf{A}^T \mathbf{q}^{(m)} - \mathbf{c}^{(m)} \\ \hline -\mathbf{L}_c^{(m)} \mathbf{c}^{(m)} \\ \mathbf{U}_c^{(m)} (\mathbf{c}^{(m)} - \mathbf{d}) \\ -\mathbf{L}_q^{(m)} (\mathbf{q}^{(m)} - \mathbf{q}_{min}) \\ \mathbf{U}_q^{(m)} (\mathbf{q}^{(m)} - \mathbf{q}_{max}) \\ \hline \mathbf{S}_s \mathbf{h}^{(m)} - \mathbf{L}_{n_v} \boldsymbol{\xi}(\mathbf{q}^{(m)}) - \mathbf{z}^{(m)} + \mathbf{L}_{z_a}^T \boldsymbol{\chi}_{z_a}^{(m)} - \mathbf{h}^s \\ \mathbf{L}_{z_a}^{(m)} \mathbf{z}^{(m)} \end{pmatrix}
\end{aligned}$$

where

$$\begin{aligned}
\delta \mathbf{q}^{(m+1)} &= \mathbf{q}^{(m+1)} - \mathbf{q}^{(m)} \\
\delta \mathbf{c}^{(m+1)} &= \mathbf{c}^{(m+1)} - \mathbf{c}^{(m)} \\
\delta \mathbf{h}^{(m+1)} &= \mathbf{h}^{(m+1)} - \mathbf{h}^{(m)} \\
\delta \boldsymbol{\lambda}^{(m+1)} &= \boldsymbol{\lambda}^{(m+1)} - \boldsymbol{\lambda}^{(m)} \\
\delta \boldsymbol{\mu}^{(m+1)} &= \boldsymbol{\mu}^{(m+1)} - \boldsymbol{\mu}^{(m)} . \\
\delta \boldsymbol{\kappa}^{(m+1)} &= \boldsymbol{\kappa}^{(m+1)} - \boldsymbol{\kappa}^{(m)} \\
\delta \boldsymbol{\nu}^{(m+1)} &= \boldsymbol{\nu}^{(m+1)} - \boldsymbol{\nu}^{(m)} \\
\delta \mathbf{z}^{(m+1)} &= \mathbf{z}^{(m+1)} - \mathbf{z}^{(m)} \\
\delta \boldsymbol{\chi}_{z_a}^{(m+1)} &= \boldsymbol{\chi}_{z_a}^{(m+1)} - \boldsymbol{\chi}_{z_a}^{(m)}
\end{aligned}$$

The Index Sets

It is necessary to define index sets which separate those links and nodes for which the constraints are saturated from those at which they are not. The index sets described in this section extend the corresponding definitions in (Piller et al. 2020) to include the local valve head loss variables, \mathbf{z} .

Let N_q be the index set of links with flow constraints, N_c be the set of all nodes with unknown-head and $d_i > 0$ and let N_v denote the index set of links which have a PRV. Eight index sets are defined: three, \mathcal{I}_{q_b} , \mathcal{I}_{q_l} , and \mathcal{I}_{q_u} , for the links which are flow constrained and three, \mathcal{I}_{c_b} , \mathcal{I}_{c_l} , and \mathcal{I}_{c_u} , which are defined only for the nodes at which the nominal demand is positive, $d_i > 0$ and two, \mathcal{I}_{z_a} , \mathcal{I}_{z_b} for the links which have PRVs. Note that membership of these sets frequently changes from one iteration to the next.

The first three sets in question are the linkflow index sets. Set \mathcal{I}_{q_b} has the indices of the links for which the flows are either in the interior of the constraint interval or have no finite constraints. The other two sets, \mathcal{I}_{q_l} and \mathcal{I}_{q_u} , hold the indices of the links for which the lower and upper bound constraints (respectively) are saturated.

The next three sets are the outflow index sets. The set \mathcal{I}_{c_b} holds the indices of the nodes at which the pressure head is between the minimum pressure head, h_m , and service pressure head h_s , and the other two sets hold the indices of the nodes at which the pressure head is either less than or equal to h_m or greater than or equal to h_s .

The last two sets contain the indices of PRV links: \mathcal{I}_{z_a} represents the indices of the links for which the z constraints are saturated (meaning $z = 0$) and \mathcal{I}_{z_b} represents the indices of the sets for which the z constraints are unsaturated (meaning $z > 0$).

The formal definitions for \mathcal{I}_{c_l} , \mathcal{I}_{c_b} , \mathcal{I}_{c_u} and \mathcal{I}_{q_l} , \mathcal{I}_{q_b} , \mathcal{I}_{q_u} (which were given previously in Piller et al. (2020)) can be found in the Supplemental Materials. The newly defined sets $\mathcal{I}_{z_b}^{(m)}$ and $\mathcal{I}_{z_a}^{(m)}$ are:

$$(a) \mathcal{I}_{z_a}^{(m)} = \{j \in N_v | (z_j < 0) \vee (z_j = 0 \wedge \chi_j \geq 0)\}$$

$$(b) \mathcal{I}_{z_b}^{(m)} = \{j \in N_v | (z_j > 0) \vee (z_j = 0 \wedge \chi_j < 0)\}$$

Thus, for PRV links, membership of \mathcal{I}_{q_b} or \mathcal{I}_{q_l} is determined entirely by whether $q > 0$ or $q = 0$. Similarly, membership of \mathcal{I}_{z_b} or \mathcal{I}_{z_a} is determined entirely by whether $z > 0$ or $z = 0$.

Denote by n_{c_l} the number of indices in \mathcal{I}_{c_l} and by n_{c_b} , n_{c_u} , n_{q_l} , n_{q_b} , n_{q_u} , n_{z_a} and n_{z_b} the corresponding numbers for the other index sets.

The rows and columns of matrices $\mathbf{M}^{(m)}$, \mathbf{I} and \mathbf{A} in (38) are now partitioned into a block three-by-three configurations. The details, which almost exactly follow the development in Piller et al. (2020), can be found in the section headed Subdivision and Analytic Reduction of the Supplemental Materials. Denote by n_{v_b} the number of PRV links that are to have their flows updated and by n_{v_l} the number of PRV links with saturated lower flow bound constraints

(i.e. which have zero flow). Denoting

$$\widehat{\mathbf{L}}_{v_b}^T = n_{q_b} \begin{pmatrix} n_{v_b} & n_{v_l} \\ \mathbf{L}_{v_b}^T & \mathbf{O} \end{pmatrix}, \quad \widehat{\mathbf{I}}_{c_b} = n_{c_b} \begin{pmatrix} n_{c_b} & n_{c_l} & n_{c_u} \\ \mathbf{I}_{c_b} & \mathbf{O} & \mathbf{O} \end{pmatrix},$$

noting that

$$\widehat{\mathbf{L}}_{v_b} \widehat{\mathbf{L}}_{v_b}^T = \begin{pmatrix} n_{v_b} & n_{v_l} \\ \mathbf{O} & \mathbf{O} \end{pmatrix} \in \mathbb{R}^{n_v \times n_v}.$$

and omitting some super- and subscripts, the resulting reduced system is given by

$$\begin{array}{c} n_{q_b} \\ n_{c_b} \\ n_j \\ n_v \\ n_{z_a} \end{array} \left(\begin{array}{ccc|cc} n_{q_b} & n_{c_b} & n_j & n_v & n_{z_a} \\ \mathbf{F}_{q_b} & \mathbf{O} & -\mathbf{A}_b & \widehat{\mathbf{L}}_{v_b}^T & \mathbf{O} \\ \mathbf{O} & \mathbf{M}_{c_b} & -\widehat{\mathbf{I}}_{c_b} & \mathbf{O} & \mathbf{O} \\ -\mathbf{A}_b^T & -\widehat{\mathbf{I}}_{c_b}^T & \mathbf{O} & \mathbf{O} & \mathbf{O} \\ \hline -\widehat{\mathbf{L}}_{v_b} \mathbf{F}_{q_b} & \mathbf{O} & \mathbf{S}_s & -\mathbf{I} & \mathbf{L}_{z_a}^T \\ \mathbf{O} & \mathbf{O} & \mathbf{O} & \mathbf{L}_{z_a} & \mathbf{O} \end{array} \right) \begin{pmatrix} \delta \mathbf{q}_b^{(m+1)} \\ \delta \mathbf{c}_b^{(m+1)} \\ \frac{\delta \mathbf{h}^{(m+1)}}{\delta \mathbf{z}^{(m+1)}} \\ \delta \boldsymbol{\chi}_{z_a}^{(m+1)} \end{pmatrix} = \quad (39)$$

$$- \begin{pmatrix} \mathbf{r}_1 \\ \mathbf{r}_2 \\ \mathbf{r}_3 \\ \mathbf{r}_4 \\ \mathbf{r}_5 \end{pmatrix} \stackrel{\text{def}}{=} - \begin{pmatrix} \mathbf{G}_{q_b} \mathbf{q}_b^{(m)} + \mathbf{L}_{v_b}^T \mathbf{z}_{v_b} - \mathbf{A}_b \mathbf{h}^{(m)} - \mathbf{a}_{q_b} \\ \mathbf{h}(\mathbf{c}_b^{(m)}) - \mathbf{h}_{c_b}^{(m)} \\ -\mathbf{A}^T \mathbf{q}^{(m)} - \mathbf{c}^{(m)} \\ \hline \mathbf{S}_s \mathbf{h}^{(m)} - \mathbf{L}_{n_v} \mathbf{G} \mathbf{q}^{(m)} - \mathbf{z}^{(m)} + \mathbf{L}_{z_a}^T \boldsymbol{\chi}_{z_a}^{(m)} - \mathbf{h}^s \\ \mathbf{L}_{z_a} \mathbf{z}^{(m)} \end{pmatrix}$$

It is worth noting here that, unlike its counterpart in (Piller et al. 2020) where only linkflows were constrained, this system is not symmetric. However, it emerges that only a small number of elements create the asymmetry. More importantly, since sparse matrix methods are typically used for the solution of the linear system, it may be that solution times for this system may be no greater than the times for similar symmetric systems where the symmetry is exploited.

A system equivalent to (39) but made up of much smaller dimension subsystems and better suited to computation is now derived. The block equations for (39) are

$$\mathbf{F}_{q_b} \delta \mathbf{q}_b^{(m+1)} - \mathbf{A}_b \delta \mathbf{h}^{(m+1)} + \widehat{\mathbf{L}}_{v_b}^T \delta \mathbf{z}^{(m+1)} = -\mathbf{r}_1 \quad (40)$$

$$\mathbf{M}_{c_b} \delta \mathbf{c}_b^{(m+1)} - \widehat{\mathbf{I}}_{c_b} \delta \mathbf{h}^{(m+1)} = -\mathbf{r}_2 \quad (41)$$

$$-\mathbf{A}_b^T \delta \mathbf{q}_b^{(m+1)} - \widehat{\mathbf{I}}_{c_b}^T \delta \mathbf{c}_b^{(m+1)} = -\mathbf{r}_3 \quad (42)$$

$$-\widehat{\mathbf{L}}_{v_b}^T \mathbf{F}_{q_b} \delta \mathbf{q}_b^{(m+1)} + \mathbf{S}_s \delta \mathbf{h}^{(m+1)} - \delta \mathbf{z}^{(m+1)} + \mathbf{L}_{z_a}^T \delta \boldsymbol{\chi}_{z_a}^{(m+1)} = -\mathbf{r}_4 \quad (43)$$

$$\mathbf{L}_{z_a} \delta \mathbf{z}^{(m+1)} = -\mathbf{r}_5 \quad (44)$$

Eq. (41) gives

$$\delta \mathbf{c}_b^{(m+1)} - \mathbf{M}_{c_b}^{-1} \widehat{\mathbf{I}}_{c_b} \delta \mathbf{h}^{(m+1)} = -\mathbf{M}_{c_b}^{-1} \mathbf{r}_2 \quad (45)$$

so

$$\widehat{\mathbf{I}}_{c_b}^T \delta \mathbf{c}_b^{(m+1)} - \widehat{\mathbf{I}}_{c_b}^T \mathbf{M}_{c_b}^{-1} \widehat{\mathbf{I}}_{c_b} \delta \mathbf{h}^{(m+1)} = -\widehat{\mathbf{I}}_{c_b}^T \mathbf{M}_{c_b}^{-1} \mathbf{r}_2$$

and adding this to (42) gives the n_j vector relation

$$-\mathbf{A}_b^T \delta \mathbf{q}_b^{(m+1)} - \widehat{\mathbf{I}}_{c_b}^T \mathbf{M}_{c_b}^{-1} \widehat{\mathbf{I}}_{c_b} \delta \mathbf{h}^{(m+1)} = -\widehat{\mathbf{I}}_{c_b}^T \mathbf{M}_{c_b}^{-1} \mathbf{r}_2 - \mathbf{r}_3 \quad (46)$$

Eq. (43) gives

$$\mathbf{L}_{z_a}^T \delta \boldsymbol{\chi}_{z_a}^{(m+1)} = \widehat{\mathbf{L}}_{v_b}^T \mathbf{F}_{q_b} \delta \mathbf{q}_b^{(m+1)} - \mathbf{S}_s \delta \mathbf{h}^{(m+1)} + \delta \mathbf{z}^{(m+1)} - \mathbf{r}_4$$

and multiplying this on the left by \mathbf{L}_{z_a} gives, noting that $\mathbf{L}_{z_a} \mathbf{L}_{z_a}^T = \mathbf{I}$ and that $\mathbf{L}_{z_a} \delta \mathbf{z}^{(m+1)}$ vanishes,

$$\delta \boldsymbol{\chi}_{z_a}^{(m+1)} = \mathbf{L}_{z_a} \left(\widehat{\mathbf{L}}_{v_b}^T \mathbf{F}_{q_b} \delta \mathbf{q}_b^{(m+1)} - \mathbf{S}_s \delta \mathbf{h}^{(m+1)} - \mathbf{r}_4 \right) \quad (47)$$

from which $\boldsymbol{\chi}_{z_a}^{(m+1)}$ can be obtained once $\delta \mathbf{q}_b^{(m+1)}$, and $\delta \mathbf{h}^{(m+1)}$ are known. Note that all the elements of $\boldsymbol{\chi}$ which are not in \mathcal{I}_{z_a} are necessarily zero by complementary slackness. Alternatively, we can rewrite (43) as

$$\delta \mathbf{z}^{(m+1)} = \mathbf{L}_{z_a}^T \delta \boldsymbol{\chi}_{z_a}^{(m+1)} - \widehat{\mathbf{L}}_{v_b}^T \mathbf{F}_{q_b} \delta \mathbf{q}_b^{(m+1)} + \mathbf{S}_s \delta \mathbf{h}^{(m+1)} + \mathbf{r}_4 \quad (48)$$

and substitute for $\delta \mathbf{z}^{(m+1)}$ in (40). This gives

$$\left(\mathbf{I}_{q_b} - \widehat{\mathbf{L}}_{v_b}^T \widehat{\mathbf{L}}_{v_b} \right) \mathbf{F}_{q_b} \delta \mathbf{q}_b^{(m+1)} + \left(\widehat{\mathbf{L}}_{v_b}^T \mathbf{S}_s - \mathbf{A}_b \right) \delta \mathbf{h}^{(m+1)} + \widehat{\mathbf{L}}_{v_b}^T \mathbf{L}_{z_a}^T \delta \boldsymbol{\chi}_{z_a}^{(m+1)} = -\widehat{\mathbf{L}}_{v_b}^T \mathbf{r}_4 - \mathbf{r}_1 \quad (49)$$

Substituting for $\delta \boldsymbol{\chi}_{z_a}^{(m+1)}$ given in (47) in (49) gives

$$\begin{aligned} & \left(\mathbf{I}_{q_b} - \widehat{\mathbf{L}}_{v_b}^T \left(\mathbf{I}_{n_v} - \mathbf{L}_{z_a}^T \mathbf{L}_{z_a} \right) \widehat{\mathbf{L}}_{v_b} \right) \mathbf{F}_{q_b} \delta \mathbf{q}_b^{(m+1)} \\ & + \left(\widehat{\mathbf{L}}_{v_b}^T \left(\mathbf{I}_{n_v} - \mathbf{L}_{z_a}^T \mathbf{L}_{z_a} \right) \mathbf{S}_s - \mathbf{A}_b \right) \delta \mathbf{h}^{(m+1)} = -\widehat{\mathbf{L}}_{v_b}^T \left(\mathbf{I} - \mathbf{L}_{z_a}^T \mathbf{L}_{z_a} \right) \mathbf{r}_4 - \mathbf{r}_1 \end{aligned}$$

Denote $\mathbf{P} = \mathbf{I}_{n_v} - \mathbf{L}_{z_a}^T \mathbf{L}_{z_a}$. This is a diagonal matrix with zeros on the diagonal where $z = 0$.

Thus,

$$\left(\mathbf{I}_{q_b} - \widehat{\mathbf{L}}_{v_b}^T \mathbf{P} \widehat{\mathbf{L}}_{v_b}\right) \mathbf{F}_{q_b} \delta \mathbf{q}_b^{(m+1)} - \left(\mathbf{A}_b - \widehat{\mathbf{L}}_{v_b}^T \mathbf{P} \mathbf{S}_s\right) \delta \mathbf{h}^{(m+1)} = -\widehat{\mathbf{L}}_{v_b}^T \mathbf{P} \mathbf{r}_4 - \mathbf{r}_1 \quad (50)$$

or, with $\widehat{\mathbf{F}}_{q_b} \stackrel{\text{def}}{=} \left(\mathbf{I}_{q_b} - \widehat{\mathbf{L}}_{v_b}^T \mathbf{P} \widehat{\mathbf{L}}_{v_b}\right) \mathbf{F}_{q_b}$ and $\widehat{\mathbf{A}} \stackrel{\text{def}}{=} \left(\mathbf{A}_b - \widehat{\mathbf{L}}_{v_b}^T \mathbf{P} \mathbf{S}_s\right)$

$$\widehat{\mathbf{F}}_{q_b} \delta \mathbf{q}_b^{(m+1)} - \widehat{\mathbf{A}} \delta \mathbf{h}^{(m+1)} = -\left(\widehat{\mathbf{L}}_{v_b}^T \mathbf{P} \mathbf{r}_4 + \mathbf{r}_1\right) \quad (51)$$

(The diagonal matrix $\widehat{\mathbf{F}}_{q_b}$ is frequently not invertible because of the zeros in the diagonal matrix $\left(\mathbf{I}_{q_b} - \widehat{\mathbf{L}}_{v_b}^T \mathbf{P} \widehat{\mathbf{L}}_{v_b}\right)$. If it is, a regularization technique which is described later can be employed. So, it is assumed, for the development, that $\widehat{\mathbf{F}}$ is invertible.) Then (51) leads to

$$\mathbf{A}_b^T \delta \mathbf{q}_b^{(m+1)} - \mathbf{A}_b^T \widehat{\mathbf{F}}_{q_b}^{-1} \widehat{\mathbf{A}} \delta \mathbf{h}^{(m+1)} = -\mathbf{A}_b^T \widehat{\mathbf{F}}^{-1} \left(\widehat{\mathbf{L}}_{v_b}^T \mathbf{P} \mathbf{r}_4 + \mathbf{r}_1\right) \quad (52)$$

Adding (52) and (46) gives

$$-\left(\mathbf{A}_b^T \widehat{\mathbf{F}}_{q_b}^{-1} \widehat{\mathbf{A}} + \widehat{\mathbf{I}}_{c_b}^T \mathbf{M}_{c_b}^{-1} \widehat{\mathbf{I}}_{c_b}\right) \delta \mathbf{h}^{(m+1)} = -\widehat{\mathbf{I}}_{c_b}^T \mathbf{M}_{c_b}^{-1} \mathbf{r}_2 - \mathbf{r}_3 - \mathbf{A}_b^T \widehat{\mathbf{F}}^{-1} \left(\widehat{\mathbf{L}}_{v_b}^T \mathbf{P} \mathbf{r}_4 + \mathbf{r}_1\right)$$

The matrices $\widehat{\mathbf{F}}_{q_b}^{-1}$ and $\mathbf{M}_{c_b}^{-1}$ play similar roles here: $\widehat{\mathbf{F}}_{q_b}^{-1}$ is the inverse of the head loss derivatives (adjusted for the links at which the z constraints are saturated and the links for which the flow constraints are not saturated) while $\mathbf{M}_{c_b}^{-1}$ is the inverse of the matrix of inverse POR derivatives. Denoting $\widehat{\mathbf{V}} \stackrel{\text{def}}{=} \mathbf{A}_b^T \widehat{\mathbf{F}}_{q_b}^{-1} \widehat{\mathbf{A}} + \widehat{\mathbf{I}}_{c_b}^T \mathbf{M}_{c_b}^{-1} \widehat{\mathbf{I}}_{c_b}$ this can be written

$$\widehat{\mathbf{V}} \delta \mathbf{h}^{(m+1)} = \mathbf{A}_b^T \widehat{\mathbf{F}}^{-1} \left(\widehat{\mathbf{L}}_{v_b}^T \mathbf{P} \mathbf{r}_4 + \mathbf{r}_1\right) + \widehat{\mathbf{I}}_{c_b}^T \mathbf{M}_{c_b}^{-1} \mathbf{r}_2 + \mathbf{r}_3 \quad (53)$$

Once $\delta \mathbf{h}^{(m+1)}$ is computed from (53) then we can compute

(a)
$$\delta \mathbf{q}_b^{(m+1)} = \widehat{\mathbf{F}}_{q_b}^{-1} \left(\widehat{\mathbf{A}} \delta \mathbf{h}^{(m+1)} - \widehat{\mathbf{L}}_{v_b}^T \mathbf{P} \mathbf{r}_4 - \mathbf{r}_1\right) \quad (54)$$

from (40),

(b) $\delta \mathbf{c}_b^{(m+1)}$ from (45),

(c) $\delta \mathbf{z}^{(m+1)}$ from (48), and

(d) $\delta \boldsymbol{\chi}^{(m+1)}$ from (47).

The Lagrange multiplier update equations come from block rows 2, 3, 5 and 6 of Eq. (S.2) in the Supplemental Materials. Block row 2

$$\mathbf{F}_{q_l} \delta \mathbf{q}_{q_l}^{(m+1)} - \mathbf{A}_l \delta \mathbf{h}^{(m+1)} - \delta \boldsymbol{\kappa}^{(m+1)} + \mathbf{L}_{v_l}^T \delta \mathbf{z}_{v_l}^{(m+1)} = -\mathbf{G}_{q_l} \mathbf{q}_{l,min}^{(m)} + \mathbf{A}_l \mathbf{h}^{(m)} - \mathbf{L}_{v_l}^T \mathbf{z}_{v_l} + \mathbf{a}_{q_l} + \boldsymbol{\kappa}^{(m)}$$

gives the $\boldsymbol{\kappa}$ update equation as

$$\boldsymbol{\kappa}^{(m+1)} = \mathbf{G}_{q_l} \mathbf{q}_{l,min}^{(m)} - \mathbf{A}_l \mathbf{h}^{(m+1)} - \mathbf{a}_{q_l} + \mathbf{L}_{v_l}^T \mathbf{z}_{v_l}^{(m+1)} \quad (55)$$

where the term $\mathbf{F}_{q_l} \delta \mathbf{q}_{q_l}^{(m+1)}$ vanishes because flows in \mathcal{I}_{q_l} are not updated. Block row 3 of Eq. (S.2) is

$$\mathbf{F}_{q_u} \delta \mathbf{q}_{q_u}^{(m+1)} - \mathbf{A}_u \delta \mathbf{h}^{(m+1)} + \delta \boldsymbol{\nu}^{(m+1)} = -\mathbf{G}_{q_u} \mathbf{q}_{u,max}^{(m)} - \mathbf{L}_{v_u}^T \mathbf{z}_{v_u} + \mathbf{A}_u \mathbf{h}^{(m)} - \mathbf{a}_{q_u} - \boldsymbol{\nu}^{(m)}$$

and it gives the $\boldsymbol{\nu}$ update equation as

$$\boldsymbol{\nu}^{(m+1)} = \mathbf{A}_u \mathbf{h}^{(m+1)} - \mathbf{G}_{q_u} \mathbf{q}_{u,max}^{(m)} - \mathbf{a}_{q_u} \quad (56)$$

where, again, the term $\mathbf{F}_{q_u} \delta \mathbf{q}_{q_u}^{(m+1)}$ vanishes because the flows in \mathcal{I}_{q_u} are not updated. Block rows 5 and 6 of Eq. (S.2) give, noting that the term multiplying \mathbf{M}_{c_l} vanishes,

$$\boldsymbol{\lambda}^{(m+1)} = h_m + \mathbf{u}_{c_l} - \mathbf{h}_{c_l}^{(m+1)} \quad \text{and} \quad \boldsymbol{\mu}^{(m+1)} = -(h_s + \mathbf{u}_{c_u} - \mathbf{h}_{c_u}^{(m+1)}) \quad (57)$$

Set Assignment Scheme

At each iteration, the links, nodes and PRVs need to be assigned to the appropriate index sets. This happens after all the decision variables and the Lagrange multipliers have been updated. Once again the scheme used here is an extension of the one given in [Piller et al. \(2020\)](#) (which is given in the Supplemental Materials). The extension in question deals with the local valve head losses z and is the following. The index k of each link with a PRV is assigned to an index set, according to the value of its local valve head loss, as follows:

- (a) If $z_k > 0$ then $k \rightarrow \mathcal{I}_{z_b}$
- (b) If $z_k < 0$ then $k \rightarrow \mathcal{I}_{z_a}$
- (c) If $z_k = 0$ then
 - (i) If $\chi_k \geq 0$ then $k \rightarrow \mathcal{I}_{z_a}$
 - (ii) otherwise $k \rightarrow \mathcal{I}_{z_b}$

IMPLEMENTATION ISSUES

Starting Values

Initial heads $\mathbf{h}^{(0)}$, link flows $\mathbf{q}^{(0)}$, nodal outflows $\mathbf{c}^{(0)}$, Lagrange multipliers $\boldsymbol{\lambda}^{(0)}$, $\boldsymbol{\mu}^{(0)}$, $\boldsymbol{\kappa}^{(0)}$, $\boldsymbol{\nu}^{(0)}$, $\boldsymbol{\chi}^{(0)}$ and the corresponding index sets \mathcal{I}_{q_b} , \mathcal{I}_{q_l} , \mathcal{I}_{q_u} , \mathcal{I}_{c_b} , \mathcal{I}_{c_l} , \mathcal{I}_{c_u} , \mathcal{I}_{z_a} , \mathcal{I}_{z_b} are required to prime the iterative process. The initial outflows for nodes with positive nominal demand, $d_i > 0$ are set to mid-interval values, $c_i = d_i/2$. The corresponding initial heads are given by the general formula $h_i^{(0)} = (h_s - h_m)\gamma^{-1}(1/2) + h_m + u_i$ for nodes not on PRV links. This translates, for particular PORs, to $h_i^{(0)} = u_i + (h_s + a_2 h_m)/a_1$ with (i) $a_1 = 2$, $a_2 = 1$ for the linear, cubic and logistic PORs; (ii) $a_1 = 3$, $a_2 = 2$ for the quadratic POR; and (iii) $a_1 = 4$, $a_2 = 3$ for the unregularized, 1-side regularized and 2-side regularized Wagner PORs (see [Deuerlein et al. \(2019\)](#) for details of these PORs).

Eq. (29) can be used to design starting values $\mathbf{z}^{(0)}$, $\boldsymbol{\chi}^{(0)}$ and the heads of nodes at the ends of PRV links, as follows. The heads of the end nodes for PRV links are given the set heads, $\mathbf{S}_e \mathbf{h}^{(0)} = \mathbf{h}^s$, the $\mathbf{z}^{(0)}$ are given the arbitrary values 5 m and consequently $\boldsymbol{\chi}^{(0)} = \mathbf{o}$ by complementary slackness. For links with a PRV, the initial flow was set arbitrarily to 5 L/s. Then $\mathbf{S}_s \mathbf{h} = \mathbf{z} + \mathbf{L}_{n_v} \boldsymbol{\xi}(\mathbf{q}^{(0)}) + \mathbf{h}^s$ for consistency with (29).

The initial flows for links which have no flow constraints are set (in SI units) to $q_i^{(0)} = \pi D_i^2/12$, (equivalent to a fluid velocity of 1/3 m/s) and the initial flows for links which have two, finite flow constraints are set to $\mathbf{q}^{(0)} = (\alpha \mathbf{q}_{min} + \beta \mathbf{q}_{max})/(\alpha + \beta)$ with $\alpha = \beta = 1$ for mid-interval initial link flows.

The initial Lagrange multipliers are set to $\lambda_i^{(0)} = \mu_i^{(0)} = \kappa_i^{(0)} = \nu_i^{(0)} = \chi_i^{(0)} = 0$, $\forall i$ and all new Lagrange multipliers are zeroed at the beginning of each iteration.

With $c_i/d_i = 1/2$ and $\alpha = \beta = 1$ the corresponding initial index sets are $\mathcal{I}_{q_b} = \{1, 2, \dots, n_p\}$, $\mathcal{I}_{c_b} = \{1, 2, \dots, n_j\}$, $\mathcal{I}_{z_b} = \{1, 2, \dots, n_v\}$, $\mathcal{I}_{c_u} = \mathcal{I}_{c_l} = \mathcal{I}_{q_u} = \mathcal{I}_{q_l} = \mathcal{I}_{z_a} = \emptyset$.

THE ITERATION LOOP

The iteration loop to implement the NEPC is now described.

- (a) Zero all the new Lagrange multipliers.
- (b) Solve Eq. (53) for the head corrections $\delta \mathbf{h}^{(m+1)}$.
- (c) Find the
 - (i) \mathcal{I}_{q_b} linkflows corrections, $\delta \mathbf{q}_b^{(m+1)}$, from (54)
 - (ii) \mathcal{I}_{c_b} outflows corrections, $\delta \mathbf{c}_b^{(m+1)}$, from (45)
 - (iii) \mathcal{I}_{z_b} local valve head loss corrections, $\delta \mathbf{z}^{(m+1)}$, from (48)
 - (iv) \mathcal{I}_{z_a} Lagrange multiplier corrections, $\delta \boldsymbol{\chi}_{z_a}^{(m+1)}$, from (47)

- (d) Compute the Lagrange multipliers, $\lambda^{(m+1)}$, $\mu^{(m+1)}$, $\kappa^{(m+1)}$, $\nu^{(m+1)}$ using (57), (55) and (56) respectively.
- (e) Assign the link, node and local valve head loss variable indices to the appropriate index sets as described in the section headed “Set Assignment”.
- (f) Project any linkflows, outflows and local valve head losses variables z which fall outside their constraint intervals to their closest boundary values:
- (i) for links with flow constraints but no PRVs
 $q^{(m+1)} \leftarrow \max(\min(q^{(m+1)}, q_{max}), q_{min})$
 - (ii) for links with PRVs $q^{(m+1)} \leftarrow \max(q^{(m+1)}, o)$
 - (iii) for nodes with positive demands $c \rightarrow \max(\min(c, d), o)$
 - (iv) local valve head loss variable $z \rightarrow \max(z, o)$

EXAMPLES AND DISCUSSION

The Local Valve Head Loss Function $f(z)$

The network in Fig. 2 serves to illustrate the behaviour of the function $f(z)$ of (6) under various head set point conditions. Fig. 6 shows the local valve head loss function $f(z)$ for three different head set point values, $h^s = 20, 40, 60$ m. For $h^s = 60$ m the PRV is fully open, for $h^s = 40$ m it is active and the minimum point is evident and for $h^s = 20$ m the PRV is fully closed.

Computational Details and Conditions

All the calculations reported in this paper were performed using the authors’ own codes written for [Matlab \(2020a\)](#) which uses IEEE standard double precision floating-point arithmetic. The tests were run on a PC with an i9-10885H CPU.

Denote the measures of the errors between successive q iterates by

$$\delta_q^{(m+1)} = \max_j \frac{|q_j^{(m+1)} - q_j^{(m)}|}{1 + |q_j^{(m+1)}|}, \quad (58)$$

with corresponding notation for the errors of the c , h and z iterates. In all cases

- (i) the 1-side regularized Wagner POR was used (see [Deuerlein et al. \(2019\)](#) for details)
- (ii) the Darcy-Weisbach head loss model was used, unless otherwise stated,

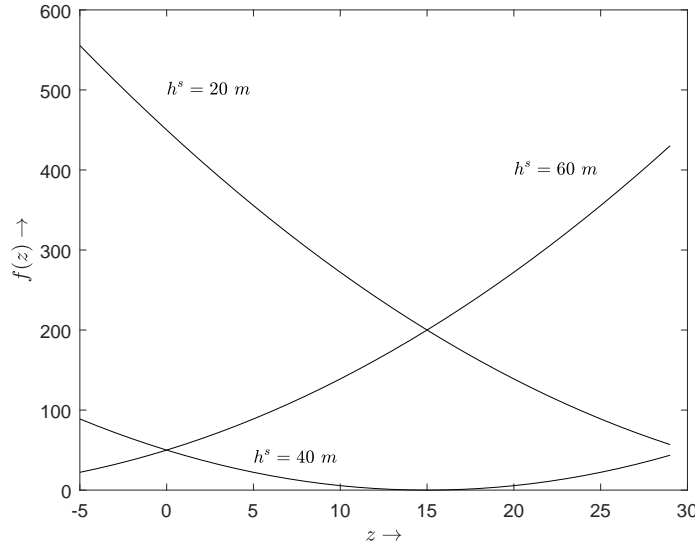


Figure 6: The local valve head loss objective function $f(z)$ for three different h^s values. For $h^s = 60$ m the PCD is fully open, for $h^s = 40$ m the PCD is active and for $h^s = 20$ m it is fully closed.

(iii) the starting scheme described above was used and

(iv) the iterations were run until (a) the relative differences between successive iterates $\delta_q^{(m+1)}$, $\delta_c^{(m+1)}$, $\delta_h^{(m+1)}$ and $\delta_z^{(m+1)}$ were smaller than the prescribed stopping tolerance $\epsilon_s = 10^{-10}$ (this stopping tolerance, even though it is smaller than would normally be used in practice, was chosen to ensure that the quadratic convergence normally associated with Newton's method was evident) or (b) the residuals were too small to make any further computation practicable because the iterative correction terms vanished.

Example 1: An FCV and PRV in Series

The network shown in Fig. 4 has an FCV and a PRV in series and is functionally very similar (within the constraints of the modelling differences) to that in Fig. 6 of Piller & van Zyl (2014) which first appeared in Simpson (1999). The head loss is modelled by the Hazen-Williams formula, all roughness coefficients are $C = 100$ and all links have diameters 500 mm. Link 1 has length 400 m, links 2 and 4 have lengths 1 m, link 3 has length 198 m and link 5 has length 600 m, giving a total network length of 1200 m. Link 2 has an FCV with flows constrained to lie in $[0, 2000]$ L/s (rendering it inactive or open) and link 4 has a PRV with $h^s = 35$ m. Node 5 has a fixed head of 60 m while node 6 has a fixed head of 30 m. Nodes 1 to 4 have zero demands and zero elevations.

The makeup of this network demonstrates that, even though controls in the NEPC are integrated into regular network links, networks can be constructed to be functionally equivalent to the networks with control valves that are modelled in EPANET.

The NEPC found the steady-state for this problem in 7 iterations. No regularization of the $\widehat{\mathbf{F}}$ matrix or the Schur complement, $\widehat{\mathbf{V}}$, was necessary. The quadratic convergence normally seen with Newton’s method was clearly evident. The linkflows (which are all equal in magnitude) were 339 L/s: the same as the figure reported in Piller & van Zyl (2014). The heads at nodes 1 and 2 were 57 m. Node 4 had the required set head of 35 m, indicating that the PRV was active, and node 3 had a set head of 55 m. The local valve head loss at steady-state was $z = 20$ m, the same as the figure reported in Piller & van Zyl (2014). The same problem, but with the Darcy-Weisbach head loss model instead, had steady-state flows of 346 L/s but all other results matched the Hazen-Williams version results.

Example 2: A Looped Network with an FCV and PRVs

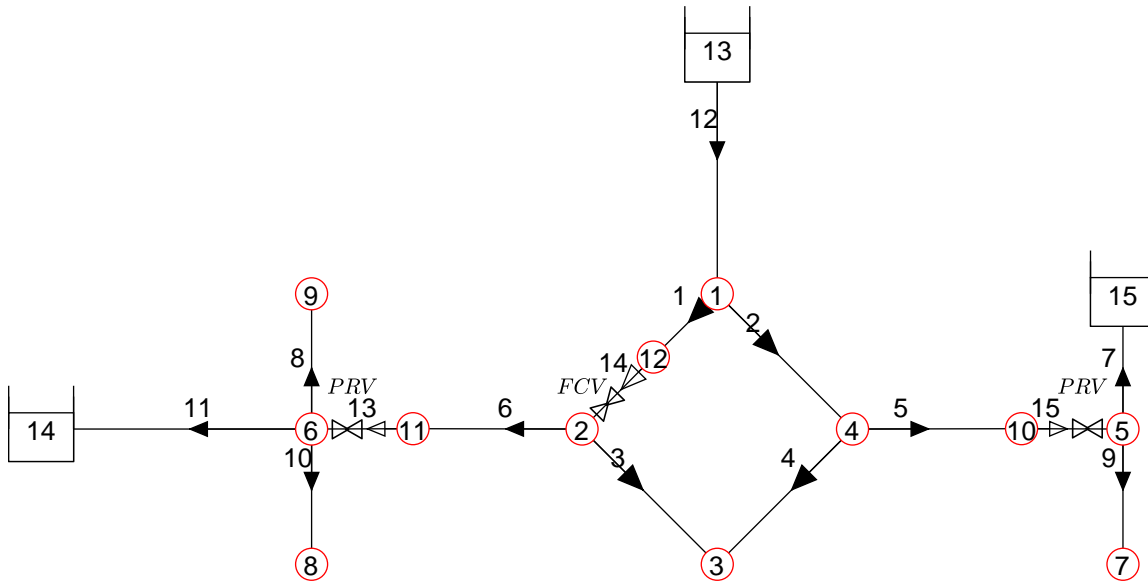


Figure 7: The illustrative looped network used to demonstrate a case with a saturated flow constraint, an active PRV and a closed PRV.

The singly-looped network shown in Fig. 7 has an FCV and two PRVs and has three nodes with fixed head: node 13 has a head of 100 m and nodes 14 and 15 have heads of 60 m. The set pressure heads of the PRVs at nodes 5 and 6 are 20 m and 55 m, respectively. These settings illustrate a case where one PRV is active, one is closed and a linkflow constraint is saturated. Table 2 shows the network links data and steady-state solutions and Table 3 shows the network node data and the steady-state solutions. At steady-state the PRV in link 13 is active with $z_{13} = 40.2$ m, $q_{13} = 16.8$ L/s, $h_6 = h_6^s = 55 + 10$ m (note that the PRV set pressure head is 55 m). This situation is depicted in Fig. C.2. The PRV in link 15 is closed with $z_{15} = 78.4$ m, $q_{15} = 0$ L/s, $h_5 = 57.1$ m, $h_5^s = 20 + 25$ m and this situation is depicted in Fig. C.3. The FCV linkflow constraint on link 14 is saturated with a linkflow of $q_{14} = q_{14,max} = 30$ L/s.

k	L_k	D_k	ϵ_r	$q_{k,min}$	q_k	$q_{k,max}$	z_k
1	2000	450	0.25	–	30.0	–	–
2	1000	450	0.25	–	76.8	–	–
3	1000	250	0.25	–	–16.8	–	–
4	1000	250	0.25	–	36.8	–	–
5	2000	375	0.25	–	–0.0	–	–
6	2000	375	0.25	–	16.8	–	–
7	1000	250	0.25	–	–40.0	–	–
8	1000	250	0.25	–	40.0	–	–
9	1000	250	0.25	–	40.0	–	–
10	1000	250	0.25	–	30.0	–	–
11	1000	250	0.25	–	–53.2	–	–
12	1000	450	0.25	–	116.8	–	–
13	0.1	375	0.25	0	16.8	–	40.2
14	0.1	450	0.25	0	30.0	30	–
15	0.1	375	0.25	0	0.0	–	78.4

Table 2: Network link and PRV parameters and solution values for the network shown in Fig. 7. The PRV in link 13 is active ($z_k = 40.2$ m, $q_5 = 16.8$ L/s) while the PRV in link 15 is closed ($z_{15} = 78.4$ m, $q_{15} = 0$ L/s). The flow constraint on link 14 is saturated ($q_{14} = q_{14,max} = 30$ L/s).

The stopping test was satisfied, for this example, after just 6 iterations and neither of the regularization schemes were invoked. The quadratic convergence associated with Newton’s method was clearly evident.

Example 3: NEPC on a Larger Network

The NEPC was applied to the case study network N_3 that the authors have used previously in [Deurerlein et al. \(2019\)](#) and elsewhere. It is essentially the Wolf-Cordera network (*Wolf-Cordera-Ranch Benchmark Example 2020*) modified to have all controls removed (see e.g. [Elhay et al. \(2021\)](#) for details). Its EPANET .inp file is available from the ASCE Library (www.ascelibrary.org). This network has $n_p = 1972$, $n_j = 1770$, $n_f = 4$. For this illustration of the NEPC, 201 linkflow constraints, which limited the linkflow to lie between zero and $\pm 10\%$ of its unconstrained value, were imposed on cotree links and 4 PRVs were situated on spanning tree links. The set pressure head values used in this case led to two of the PRVs active at steady-state and the other two fully open. The total delivery fraction was 86.3%.

The NEPC took 31 iterations to satisfy the stopping test and, as before, the quadratic

k	u_k	c_k	d_k	$\frac{c_k}{d_k} \%$	h_{jk}	h_{jk}^s
1	50	10	10	100	98.9	–
2	50	30	30	100	95.4	–
3	50	20	20	100	95.9	–
4	50	40	40	100	98.4	–
5	25	0	0	0	57.1	20 + 25
6	10	0	0	0	65.0	55 + 10
7	25	40	40	100	54.3	–
8	25	30	30	100	53.4	–
9	25	40	40	100	52.1	–
10	25	0	0	0	98.4	–
11	10	0	0	0	95.2	–
12	50	0	0	0	98.7	–

Table 3: Network node parameters and solution values for the network shown in Fig. 7. The PRV in link 13 is active ($h_6 = 55 + 10 = 65$ m) while the PRV in link 15 is closed ($h_5 = 57.1$ m, $h_5^s = 20 + 25$ m).

convergence of Newton’s method was clearly evident. Regularization of the Schur complement, $\widehat{\mathbf{V}}$, matrix was required and in one step the regularization of the $\widehat{\mathbf{F}}$ matrix was required.

CONCLUSIONS

This paper introduces a new method, the Nash Equilibrium for pressure controls, for the modelling of pressure control devices on a PDM WDS with linkflow control devices. The NEPC extends the ASM methods developed by the present authors for handling PDM systems without and with flow constraints. An ASM for WDSs without flow control devices was used to solve a content-based, linear-equality constrained optimization problem while an ASM for WDSs with flow control devices was used to solve an optimization problem with linear equality and linear box constraints. In both these cases the solution heads were the Lagrange multipliers of the linear equality constraints. However, modelling the control of system heads cannot be achieved simply by imposing constraints on the Lagrange multipliers. Instead the problem is formulated as a competitive game between many players: one player for each of the n_v PRVs and one player for the rest of the system. Each PRV player tries to optimize a new unknown, z_k , known as its local valve head loss, using only local information and treating the linkflows and outflows as parameters. By contrast the linkflows and outflows are found from the minimization of the system’s content function, which incorporates the local valve head losses as parameters. The solution to the problem is the game’s Nash Equilibrium, the steady-state at which none

of the players can improve their position by unilaterally changing strategy. In the NEPC the PRVs are located next to the node at the downstream end of a normal link, the PRV node. The process can be viewed as simply adding a PRV to an existing link in a network: the link properties (length, diameter, roughness) remain unchanged. It is assumed that (i) no link in the network has both a PRV and an FCV, (ii) the PRV node has zero demand (iii) there is always a path with unsaturated links between the PRV link's upstream node and a source. The Nash Equilibrium is found as the solution of the KKT conditions that follow from the characterisation of the joint optimization problems. The Newton method for this reliably finds the solution rapidly and is demonstrated on some small illustrative examples (including one with results that duplicate the results of an example in the literature) and a larger network with about 2,000 links and 1,800 nodes that is familiar in the literature. It is important to note that even though PRVs in the NEPC are integrated into regular network links, networks can be constructed to be functionally very similar to the networks with controls as they are modelled in EPANET.

The new method uses a comprehensive model that includes FCVs and PRVs together. The states of the control devices is always known without, as in previously published methods, using any heuristics such as those which require having to interrogate the valve states at each iteration.

Water engineers well know that care must be exercised in the placement of pressure and flow control devices in real WDSs. Similarly, care must be exercised in their models. Restricting links with flow constraints to the cotree and links with pressure controls to the spanning tree is one precaution that, although it may not always be desirable, can be taken. It will avoid violating the LICQ. In any case, the flow direction of a PRV needs to be from the root to the leaves of the spanning tree. The assumption that PRV nodes have zero demands will also avoid the possibility that two active constraints conflict, again avoiding a violation of the LICQ.

While this proof-of-concept paper details how to model PRVs, this modelling framework is equally applicable to PSVs and variable speed pumps for pressure control without essential modification.

Larger networks with pressure and flow controls are no more difficult to solve by the new method than small-to-medium networks. The size of the network does not, in the authors' experience, appear to change the problem's difficulty.

There are several questions that naturally arise from the work in this paper.

- (a) It would be interesting to know if the asymmetry in this problem confers any serious disadvantage in large networks given that (i) sparse matrix arithmetic is used, (ii) the closeness to symmetry of the key matrix involved.
- (b) A key question in ASMs centers on what to do in case the LICQ is violated. If the

violation occurs at the solution, the problem has no unique solution because the Lagrange multipliers are not unique. If the violation is only at a point on the way to the solution then to continue requires the identification of which of the active constraints should be relaxed. This process can be very costly computationally and new ways to address this problem efficiently and quickly are needed.

- (c) If there are flow constraints on every link in a network, as in capacity testing (e.g. determining maximum transport flows in all network links), then only the constraints on a cotree can saturate without isolating some nodes. Determining which is the appropriate cotree for this situation is difficult and when pressure controls are added, the problem is even more difficult.

APPENDIX A

There are two instances where the NEPC may require regularization: (i) the diagonal matrix of head loss derivatives, $\widehat{\mathbf{F}}_{q_b}$, may have zeros on the diagonal, and (ii) the Schur complement, $\widehat{\mathbf{V}}$, of (53) can become singular if the matrix $\widehat{\mathbf{A}}$ of (51) has less than full rank because of the particular membership of the index set \mathcal{I}_{q_b} at that point. Regularization schemes for these singularities are now described.

$$\text{Regularization of } \widehat{\mathbf{F}}_{q_b} = \left(\mathbf{I}_{q_b} - \widehat{\mathbf{L}}_{v_b}^T \mathbf{P} \widehat{\mathbf{L}}_{v_b} \right) \mathbf{F}_{q_b}$$

The matrix $\widehat{\mathbf{F}}$ will be singular whenever links with PRVs fall into the intersection $\mathcal{I}_{q_b} \cap \mathcal{I}_{z_b}$, i.e. whenever the valve status is active (or the z constraint is unsaturated, $q > 0$, and $z > 0$) because then the term $\left(\mathbf{I}_{q_b} - \widehat{\mathbf{L}}_{v_b}^T \mathbf{P} \widehat{\mathbf{L}}_{v_b} \right)$ is an identity with zeros where the row corresponds to the PRV link. A regularization scheme which addresses this is now described.

Suppose the Newton iteration for a saddle point system is

$$\begin{pmatrix} \mathbf{D}^{(m)} & -\mathbf{A} \\ -\mathbf{A}^T & \mathbf{E}^{(m)} \end{pmatrix} \begin{pmatrix} \delta \mathbf{x}_1^{(m+1)} \\ \delta \mathbf{x}_2^{(m+1)} \end{pmatrix} = - \begin{pmatrix} \mathbf{b}_1 \\ \mathbf{b}_2 \end{pmatrix} \quad (\text{A.1})$$

\mathbf{D} diagonal and singular, where $\delta \mathbf{x}^{(m+1)} = \mathbf{x}^{(m+1)} - \mathbf{x}^{(m)}$. Then (A.1) can be written

$$\begin{pmatrix} \mathbf{D}^{(m)} & -\mathbf{A} \\ -\mathbf{A}^T & \mathbf{E}^{(m)} \end{pmatrix} \begin{pmatrix} \mathbf{x}_1^{(m+1)} \\ \mathbf{x}_2^{(m+1)} \end{pmatrix} = \begin{pmatrix} \mathbf{D}^{(m)} & -\mathbf{A} \\ -\mathbf{A}^T & \mathbf{E}^{(m)} \end{pmatrix} \begin{pmatrix} \mathbf{x}_1^{(m)} \\ \mathbf{x}_2^{(m)} \end{pmatrix} - \begin{pmatrix} \mathbf{b}_1 \\ \mathbf{b}_2 \end{pmatrix} \quad (\text{A.2})$$

In the limit

$$\begin{pmatrix} \mathbf{D} & -\mathbf{A} \\ -\mathbf{A}^T & \mathbf{E} \end{pmatrix} \begin{pmatrix} \mathbf{x}_1 \\ \mathbf{x}_2 \end{pmatrix} = \begin{pmatrix} \mathbf{D} & -\mathbf{A} \\ -\mathbf{A}^T & \mathbf{E} \end{pmatrix} \begin{pmatrix} \mathbf{x}_1 \\ \mathbf{x}_2 \end{pmatrix} - \begin{pmatrix} \mathbf{b}_1 \\ \mathbf{b}_2 \end{pmatrix} \quad (\text{A.3})$$

and for diagonal \mathbf{T} , which is conformal with \mathbf{D} ,

$$\begin{pmatrix} \mathbf{D} + \mathbf{T} & -\mathbf{A} \\ -\mathbf{A}^T & \mathbf{E} \end{pmatrix} \begin{pmatrix} \mathbf{x}_1 \\ \mathbf{x}_2 \end{pmatrix} = \begin{pmatrix} \mathbf{D} + \mathbf{T} & -\mathbf{A} \\ -\mathbf{A}^T & \mathbf{E} \end{pmatrix} \begin{pmatrix} \mathbf{x}_1 \\ \mathbf{x}_2 \end{pmatrix} - \begin{pmatrix} \mathbf{b}_1 \\ \mathbf{b}_2 \end{pmatrix} \quad (\text{A.4})$$

which suggests the fixed point iteration

$$\begin{pmatrix} \mathbf{D}^{(m)} + \mathbf{T}^{(m)} & -\mathbf{A} \\ -\mathbf{A}^T & \mathbf{E}^{(m)} \end{pmatrix} \begin{pmatrix} \mathbf{x}_1^{(m+1)} \\ \mathbf{x}_2^{(m+1)} \end{pmatrix} = \begin{pmatrix} \mathbf{D}^{(m)} + \mathbf{T}^{(m)} & -\mathbf{A} \\ -\mathbf{A}^T & \mathbf{E}^{(m)} \end{pmatrix} \begin{pmatrix} \mathbf{x}_1^{(m)} \\ \mathbf{x}_2^{(m)} \end{pmatrix} - \begin{pmatrix} \mathbf{b}_1 \\ \mathbf{b}_2 \end{pmatrix} \quad (\text{A.5})$$

This can also be written

$$\begin{pmatrix} \mathbf{D}^{(m)} + \mathbf{T}^{(m)} & -\mathbf{A} \\ -\mathbf{A}^T & \mathbf{E}^{(m)} \end{pmatrix} \begin{pmatrix} \delta \mathbf{x}_1^{(m+1)} \\ \delta \mathbf{x}_2^{(m+1)} \end{pmatrix} = - \begin{pmatrix} \mathbf{b}_1 \\ \mathbf{b}_2 \end{pmatrix} \quad (\text{A.6})$$

In order to limit the condition of \mathbf{D} (which is infinite if it is not invertible) to some constant y , it is only necessary that any term on the diagonal of \mathbf{D} smaller than $\tau = \max_i[\mathbf{D}]_{ii}/|y|$ be replaced by τ . The Newton iteration (A.1) has, in general, quadratic convergence in the vicinity of a solution point. The fixed point iteration, (A.6), while it is no longer a true Newton method, frequently has close to quadratic convergence for small \mathbf{T} . This scheme, introduced in (Elhay & Simpson 2011), has been used with success to address the singularity or poor condition of the matrix $\widehat{\mathbf{F}}_{q_b}$ in the NEPC.

Regularization of the Schur Complement, $\widehat{\mathbf{V}}$

Denote $\mathcal{I}_{q_{lu}} = \mathcal{I}_{q_l} \cup \mathcal{I}_{q_u}$ and $\mathbf{B} = \mathbf{A}(\mathcal{I}_{q_{lu}}, :)$. Adding a small factor, $\alpha \mathbf{B}^T \mathbf{B}$, to $\widehat{\mathbf{V}}$ if it has less than full rank because the membership of \mathcal{I}_{q_b} has rendered \mathbf{A}_b rank deficient has proved to be a very satisfactory regularization scheme. In all the cases reported here that required regularization, the reducing value of α was negligible by the time the stopping test was satisfied.

APPENDIX B

Nash Equilibrium Example Analysis

The brief analysis which underpins the small illustrative best reply functions example associated with Fig. 3 is presented here. Note that the resistance factors r depend on q for the Darcy-Weisbach head loss model but are independent of q for the Hazen-Williams head loss model.

The energy equations, incorporating the local valve head loss associated with the PRV, for the network in Fig. 2 are

$$rq|q|^{\eta-1} - h_1 + h_2 + z = 0 \quad (\text{B.1})$$

$$rq|q|^{\eta-1} + h_1 - h_3^0 = 0 \quad (\text{B.2})$$

$$-rq|q|^{\eta-1} + h_2 - h_4^0 = 0 \quad (\text{B.3})$$

and the equation modelling the local optimization problem for the PRV local valve head loss in link 2 (with χ the Lagrange multiplier for the z constraint) is

$$-rq|q|^{\eta-1} + h_1 - z + \chi - h^s = 0. \quad (\text{B.4})$$

From (B.2) and (B.3)

$$h_1 = h_3^0 - rq|q|^{\eta-1}, \quad h_2 = h_4^0 + rq|q|^{\eta-1}$$

and substituting these into (B.1) gives

$$3rq|q|^{\eta-1} - h_3^0 + h_4^0 + z = 0 \Rightarrow 3rq|q|^{\eta-1} = h_3^0 - h_4^0 - z$$

from which Eq. (3) follows when $\eta = 2$ and remembering that $q \geq 0$. Eq. (B.4) gives, for $z > 0$ (the complementary slackness condition is $z\chi = 0$),

$$rq|q|^{\eta-1} = h_1 - z - h^s \Rightarrow rq|q|^{\eta-1} = h_3^0 - rq|q|^{\eta-1} - z - h^s$$

from which Eq. (4), for $\eta = 2$, follows.

APPENDIX C

Illustrations of Possible Pressure Reducing Valve States

Figures C.1–C.5 show link and node parameter values for various PRV states.

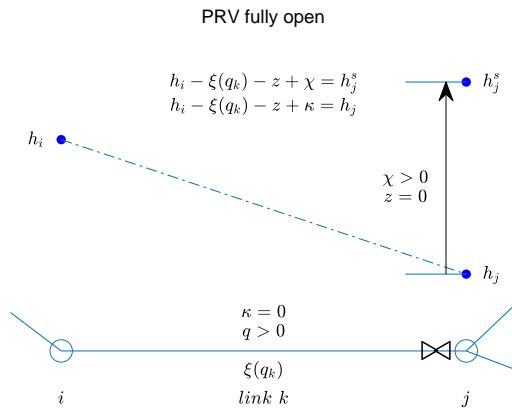


Figure C.1: Illustration of the values of various link and node parameters for PRV: fully open state

DATA AVAILABILITY STATEMENT

EPANET .inp files for the networks shown in Fig. 2, Fig. 4 and Fig. 7 together with the

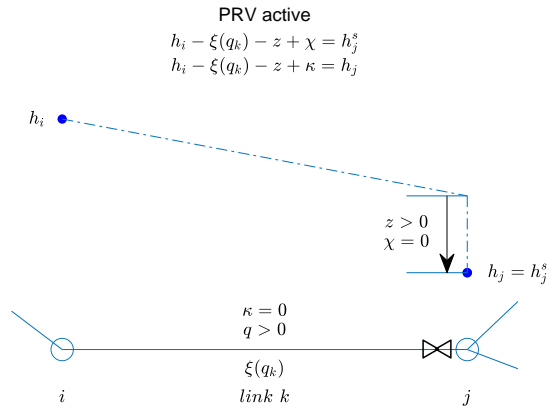


Figure C.2: Illustration of the values of various link and node parameters for PRV: active state

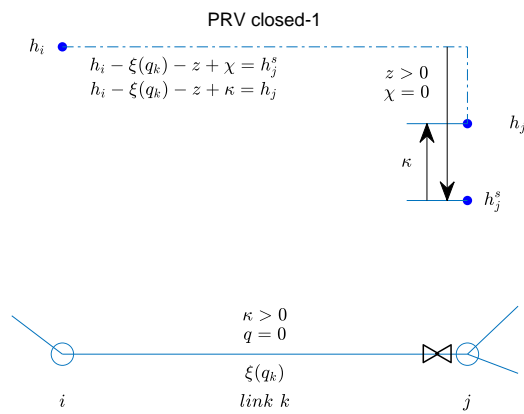


Figure C.3: Illustration of the values of various link and node parameters for PRV: closed 1 state

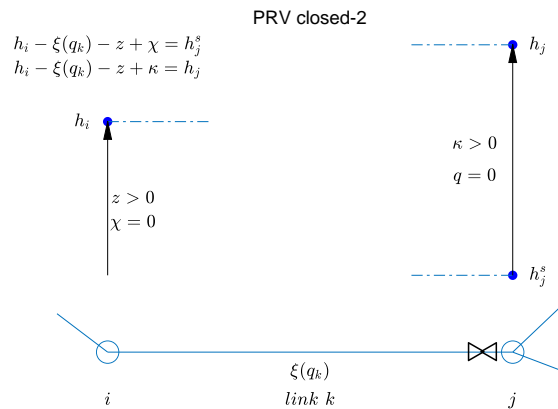


Figure C.4: Illustration of the values of various link and node parameters for PRV: closed 2 state

flow and pressure constraint definitions used in the tests reported here (FCVs and PRVs) are available from the ASCE library (www.ascelibrary.org) as Supplemental Material for this paper. An EPANET .inp file for the network of Ex. 3 is available from the ASCE library as

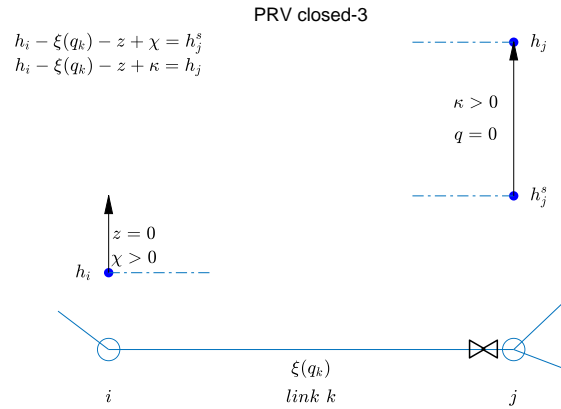


Figure C.5: Illustration of the values of various link and node parameters for PRV: closed 3 state

Supplemental Material for the paper [Deuerlein et al. \(2019\)](#).

ACKNOWLEDGMENTS

This work was supported in part by the German Ministry for Education and Research (BMBF Project W-Net 4.0 02WIK1477C).

References

- Abraham, E., Blokker, M. & Stoianov, I. (2018), ‘Decreasing the discoloration risk of drinking water distribution systems through optimized topological changes and optimal flow velocity control’, *J. Water Resour. Plann. Manage.* **144**(2), 04017093.
- Alvarruiz, F., Martinez-Alzamora, F. & Vidal, A. M. (2015), ‘Improving the efficiency of the loop method for the simulation of water distribution systems’, *J. Water Resour. Plann. Manage.* **141**(10), 04015019.
- Alvarruiz, F., Martinez-Alzamora, F. & Vidal, A. M. (2018), ‘Efficient modeling of active control valves in water distribution systems using the loop method’, *J. Hydraul. Eng.* **144**(10), 04018064. DOI: 10.1061/(ASCE)WR.1943-5452.0000982.
- Bhave, P. R. (1981), ‘Node flow analysis distribution systems’, *Transportation Engineering Journal* **107**(4), 457–467.
- Bonanno, G. (2018), *Game Theory*, CreateSpace Independent Publishing Platform.

- Collins, M., Cooper, L., Helgason, R., Kennington, J. & LeBlanc, L. (1978), ‘Solving the pipe network analysis problem using optimization techniques’, *Management Science* **24**(7), 747–760.
- Cross, H. (1936), ‘Analysis of flow in networks of conduits or conductors’, *Bulletin 266 University of Illinois Engineering Experimental Station* .
- Deuerlein, J., Piller, O., Elhay, S. & Simpson, A. R. (2019), ‘A content-based active set method for the pressure dependent model of water distribution systems’, *J. Water Resour. Plann. Manage.* **145**(1), 04018082. DOI: 10.1061/(ASCE)WR.1943-5452.0001003.
- Deuerlein, J. W. (2002), On the hydraulic system analysis of water supply networks (in German), PhD thesis, Department of Civil Engineering, Geo- and Environmental Sciences, University of Karlsruhe (TH). In German.
- Deuerlein, J. W., Cembrowicz, R. G. & Dempe, S. (2005), Hydraulic simulation of water supply networks under control. 7th Water Distribution System Analysis Conference WDSA2005.
- Elhay, S., Piller, O., Deuerlein, J. & Simpson, A. (2021), ‘An interior point method applied to flow constraints in a pressure dependent water distribution system’, *J. Water Resour. Plann. Manage.* pp. 04021090–1 – 04021090–15. DOI: 10.1061/(ASCE)WR.1943-5452.0001484.
- Elhay, S. & Simpson, A. R. (2011), ‘Dealing with zero flows in solving the non-linear equations for water distribution systems’, *J. Hydraul. Eng.* **137**(10), 1216–1224. DOI:10.1061/(ASCE)HY.1943-7900.0000411. ISSN: 0733-9429.
- Estrada, C., González, C., Aliod, R. & Paño, J. (2009), ‘Improved pressurized pipe network hydraulic solver for applications in irrigation systems’, *J. Irrig. Drain. Eng.* **135**(4), 421–430.
- Foglianti, G., Alvisi, S., Franchini, M. & Todini, E. (2020), ‘Extending the global-gradient algorithm to solve pressure-control valves’, *J. Water Resour. Plann. Manage.* **146**(8), 04020055.
- Friedman, J. W. (1986), *Game theory with applications to economics*, Oxford University Press, Oxford. ISBN 0-19-503660-3.
- Gorev, N. B., Gorev, V. N., Kodzhespriova, I. F., Shedlovsky, I. A. & Sivakumar, P. (2018), ‘Simulating control valves in water distribution systems as pipes of variable resistance’, *J. Water Resour. Plann. Manage.* **144**(11), 06018008.
- Hager, W. & Zhang, H. (2006), ‘A new active set method for box constrained optimization’, *SIAM J. Optim.* **17**(2), 526–557.

- Jun, L. & Guoping, Y. (2013), ‘Iterative methodology of pressure-dependent demand based on EPANET for pressure-deficient water distribution analysis’, *J. Water Resour. Plann. Manage.* **139**(1), 34–44. DOI: 10.1061/(ASCE)WR.1943-5452.0000227.
- Lippai, I. & Wright, L. (2014), ‘Demand constructs for risk analysis’, *Procedia Engineering* **89**, 640–647. 16th Water Distribution System Analysis Conference, WDSA2014 Urban Water Hydroinformatics and Strategic Planning.
- Mahmoud, H., Savic, D. & Kapelan, Z. (2017), ‘New pressure-driven approach for modeling water distribution networks’, *J. Water. Resour. Plann. Manage.* **143**(8), 4017031. DOI: 10.1061/(ASCE)WR.1943-5452.0000781.
- Martin, D. & Peters, G. (1963), ‘The application of Newton’s method to network analysis by digital computer’, *Journal of Institution of Water Engineers and Scientists* pp. 115–129.
- Matlab (2020a), *version 9.8.0.1359463 (R2020a) Update 1*, The MathWorks Inc., Natick, Massachusetts.
- Osborne, M. & Rubinstein, A. (1994), *A Course in Game Theory*, The MIT Press, Cambridge, Massachusetts.
- Piller, O., Deuerlein, J. W., Elhay, S. & Simpson, A. R. (2022), Which flow and pressure constraints are required for sustainable operation of water distribution systems?, in ed., ‘2nd WDSA/CCWI 2022: Joint Conference on Water Distribution and Systems Analysis & Computing and Control for the Water Industry’, DOI:10.4995/WDSA-CCWI2022.2022.14753.
- Piller, O., Elhay, S., Deuerlein, J. & Simpson, A. R. (2020), ‘A content-based active set method for the pressure dependent model of water distribution systems with flow controls’, *J. Water Resour. Plann. Manage.* **146**(4), 04020009.
- Piller, O. & van Zyl, J. E. (2014), ‘Modeling control valves in water distribution systems using a continuous state formulation’, *J. Hydraul. Eng.* **140**(11), 04014052.
- Rockafellar, R. T. (1970), *Convex Analysis*, Princeton University Press, Princeton, NJ.
- Rossman, L., Woo, H., Tryby, M., Shang, F., Janke, R. & Haxton, T. (2020), *EPANET 2.2 User’s Manual*, United States Environmental Protection Agency.
- Simpson, A. R. (1999), Modeling of pressure regulating devices – a major problem yet to be satisfactorily solved in hydraulic simulation, ASCCE. Water Distribution Systems Conference.

- Tabesh, M. (1998), Implications of the Pressure Dependency of Outflows on Data Management, Mathematical Modelling and Reliability Assesment of Water Distribution Systems, PhD, Department of Civil Engineering, University of Liverpool, UK.
- Todini, E., Farina, A., Gabriele, A., Gargano, R. & Rossman, L. (2022), ‘Comparing alternative PDA solvers with EPANET’, *Journal of Hydroinformatics* .
- Todini, E. & Pilati, S. (1988), *A gradient algorithm for the analysis of pipe networks.*, John Wiley and Sons, London, pp. 1–20.
- Wolf-Cordera-Ranch Benchmark Example* (2020), University of Exeter, Centre for Water Systems. Available from <https://emps.exeter.ac.uk/engineering/research/cws/resources/benchmarks/expansion/wolf-cordera-ranch.php>.
- Wood, D. & Charles, C. (1972), ‘Hydraulic network analysis using linear theory’, *Journal of the Hydraulics Division* **98**(7), 1157–1170.
- Wu, Z., M., T., Todini, E. & Walski, T. (2009), ‘Modeling variable-speed pump operations for target hydraulic characteristics’, *J. Am. Water Works Assoc.* **101**(1), 54–64.

SUPPLEMENTAL MATERIALS

Subdivision and Analytical Reduction of the Main System

The matrix $\mathbf{M}^{(m)}$ has three diagonal blocks: (i) the block $\mathbf{M}_{c_b}^{(m)}$ which represents those nodes at which the head lies between the minimum and service pressure head, (ii) the block $\mathbf{M}_{c_l}^{(m)}$ which represents the nodes at which the lower bound constraint is saturated and no outflow is possible because the pressure is below the minimum pressure head and (iii) the block $\mathbf{M}_{c_u}^{(m)}$ which represents the nodes at which the upper bound constraint is saturated and the outflow is at the nominal demand, d , because the head is at least at the service pressure head level:

$$\mathbf{M}^{(m)} = \begin{matrix} & n_{c_b} & n_{c_l} & n_{c_u} \\ \begin{matrix} n_{c_b} \\ n_{c_l} \\ n_{c_u} \end{matrix} & \begin{pmatrix} \mathbf{M}_{c_b}^{(m)} & & \\ & \mathbf{M}_{c_l}^{(m)} & \\ & & \mathbf{M}_{c_u}^{(m)} \end{pmatrix} \end{matrix}$$

The ANIM, \mathbf{A} is similarly partitioned into block three-by-three form where the block's first subscript refers to rows (links) sets and the second subscript refers to columns (nodes) sets: the subscripts indicate (i) the set for which the constraints are not saturated, b , (ii) the set for which the lower constraint is saturated, l , and (iii) the set for which the upper constraint is saturated, u .

$$\mathbf{A} = \begin{matrix} & n_{c_b} & n_{c_l} & n_{c_u} \\ \begin{matrix} n_{q_b} \\ n_{q_l} \\ n_{q_u} \end{matrix} & \begin{pmatrix} \mathbf{A}_{bb} & \mathbf{A}_{bl} & \mathbf{A}_{bu} \\ \mathbf{A}_{lb} & \mathbf{A}_{ll} & \mathbf{A}_{lu} \\ \mathbf{A}_{ub} & \mathbf{A}_{ul} & \mathbf{A}_{uu} \end{pmatrix} \end{matrix} = \begin{pmatrix} \mathbf{A}_{.b} \\ \mathbf{A}_{.l} \\ \mathbf{A}_{.u} \end{pmatrix} \quad (\text{S.1})$$

Note that

$$\mathbf{A}^T = \begin{matrix} & n_{q_b} & n_{q_l} & n_{q_u} \\ \begin{matrix} n_{c_b} \\ n_{c_l} \\ n_{c_u} \end{matrix} & \begin{pmatrix} \mathbf{A}_{bb}^T & \mathbf{A}_{lb}^T & \mathbf{A}_{ub}^T \\ \mathbf{A}_{bl}^T & \mathbf{A}_{ll}^T & \mathbf{A}_{ul}^T \\ \mathbf{A}_{bu}^T & \mathbf{A}_{lu}^T & \mathbf{A}_{uu}^T \end{pmatrix} \end{matrix} = \begin{pmatrix} \mathbf{A}_{.b}^T \\ \mathbf{A}_{.l}^T \\ \mathbf{A}_{.u}^T \end{pmatrix}$$

Thus, $\mathbf{A}_{bl} \in \mathbb{R}^{n_{q_b} \times n_{c_l}}$ represents those links for which the link flows are between the upper and lower constraint boundaries and the nodes for which the pressure heads are below the minimum pressure head. The various identity matrix partition blocks are designated by \mathbf{I}_q for link flows and \mathbf{I}_c for outflows.

Denote by \mathbf{L}_{+0} the selection matrix for the links in $\mathcal{I}_{q_b} \cap \mathcal{I}_{z_a}$ ($q > 0$ and $z = 0$) and denote by \mathbf{L}_{00} the selection matrix of the links in $\mathcal{I}_{q_l} \cap \mathcal{I}_{z_a}$ ($q = 0$ and $z = 0$). Denote by z_{+0} and z_{00}

the corresponding z values that are 0.

The selection matrix $\mathbf{L}_{v_b} \in \mathbb{R}^{n_{v_b} \times n_{q_b}}$ picks out the links in \mathcal{I}_{q_b} which have PRVs. A similar definition applies for $\mathbf{L}_{v_l} \in \mathbb{R}^{n_{v_l} \times n_{q_l}}$. The selection matrix $\mathbf{L}_{z_b} \in \mathbb{R}^{n_{z_b} \times n_{v_b}}$ picks out the links in \mathcal{I}_{q_b} which have PRVs for which $z > 0$. A similar definition applies for $\mathbf{L}_{z_a} \in \mathbb{R}^{n_{z_a} \times n_{v_l}}$.

Denote by \mathbf{z}_{+0} the z values for links with $q > 0$ and $z = 0$ and by \mathbf{z}_{00} the z values for links with $q = 0$ and $z = 0$. Together they comprise all the PRV links with $z = 0$, i.e the set \mathcal{I}_{z_a} .

If the matrix $\mathbf{G}^{(m)}$, the head loss derivatives matrix $\mathbf{F}^{(m)}$ and the identity are partitioned conformally with $\mathbf{M}^{(m)}$ and \mathbf{A} the resulting system is

$$\begin{pmatrix}
\delta \mathbf{q}_b^{(m+1)} \\
\delta \mathbf{q}_l^{(m+1)} \\
\delta \mathbf{q}_u^{(m+1)} \\
\delta \mathbf{c}_b^{(m+1)} \\
\delta \mathbf{c}_l^{(m+1)} \\
\delta \mathbf{c}_u^{(m+1)} \\
\delta \mathbf{h}_{c_b}^{(m+1)} \\
\delta \mathbf{h}_{c_l}^{(m+1)} \\
\delta \mathbf{h}_{c_u}^{(m+1)} \\
\delta \boldsymbol{\lambda}^{(m+1)} \\
\delta \boldsymbol{\mu}^{(m+1)} \\
\delta \boldsymbol{\kappa}^{(m+1)} \\
\delta \boldsymbol{\nu}^{(m+1)} \\
\delta \mathbf{z}_{v_b}^{(m+1)} \\
\delta \mathbf{z}_{v_l}^{(m+1)} \\
\delta \boldsymbol{\chi}_{+0}^{(m+1)} \\
\delta \boldsymbol{\chi}_{00}^{(m+1)}
\end{pmatrix}
= -
\begin{pmatrix}
\mathbf{G}_{q_b} \mathbf{q}_b^{(m)} + \mathbf{L}_{v_b}^T \mathbf{z}_{v_b} - \mathbf{A}_b \mathbf{h}^{(m)} - \mathbf{a}_{q_b} \\
\mathbf{G}_{q_l} \mathbf{q}_l^{(m)} + \mathbf{L}_{v_l}^T \mathbf{z}_{v_l} - \mathbf{A}_l \mathbf{h}^{(m)} - \mathbf{a}_{q_l} - \boldsymbol{\kappa}^{(m)} \\
\mathbf{G}_{q_u} \mathbf{q}_u^{(m)} - \mathbf{A}_u \mathbf{h}^{(m)} - \mathbf{a}_{q_u} + \boldsymbol{\nu}^{(m)} \\
\hline
\mathbf{h}(\mathbf{c}_b^{(m)}) - \mathbf{h}_{c_b}^{(m)} \\
-\mathbf{h}_{c_l}^{(m)} + h_m + \mathbf{u}_{c_l} - \boldsymbol{\lambda}^{(m)} \\
-\mathbf{h}_{c_u}^{(m)} + h_s + \mathbf{u}_{c_u} + \boldsymbol{\mu}^{(m)} \\
\hline
-\mathbf{A}_{.b}^T \mathbf{q}^{(m)} - \mathbf{c}_b^{(m)} \\
-\mathbf{A}_{.l}^T \mathbf{q}^{(m)} - \mathbf{c}_l^{(m)} \\
-\mathbf{A}_{.u}^T \mathbf{q}^{(m)} - \mathbf{c}_u^{(m)} \\
\hline
-\mathbf{c}_l^{(m)} \\
\mathbf{c}_u^{(m)} - \mathbf{d}_u \\
-\mathbf{q}_l^{(m)} + \mathbf{q}_{l,min} \\
\mathbf{q}_u^{(m)} - \mathbf{q}_{u,max} \\
\hline
\mathbf{L}_{v_b} \left(\mathbf{S}_s \mathbf{h}^{(m)} - \mathbf{L}_{n_v} \boldsymbol{\xi}(\mathbf{q}^{(m)}) - \mathbf{z}^{(m)} + \boldsymbol{\chi}^{(m)*} - \mathbf{h}^s \right) \\
\mathbf{L}_{v_l} \left(\mathbf{S}_s \mathbf{h}^{(m)} - \mathbf{L}_{n_v} \boldsymbol{\xi}(\mathbf{q}^{(m)}) - \mathbf{z}^{(m)} + \boldsymbol{\chi}^{(m)*} - \mathbf{h}^s \right) \\
\hline
\mathbf{z}_{+0}^{(m)} \\
\mathbf{z}_{00}^{(m)}
\end{pmatrix}$$

It is possible to analytically eliminate some of the equations in the system (S.2).

Block row 12 of (S.2) is $-\delta \mathbf{q}_l^{(m+1)} \stackrel{\text{def}}{=} -\mathbf{q}_l^{(m+1)} + \mathbf{q}_l^{(m)} = \mathbf{q}_l^{(m)} - q_{l,min}$ giving $\mathbf{q}_l^{(m+1)} = q_{l,min}$. Similarly, block row 13 is $\mathbf{q}_u^{(m+1)} - \mathbf{q}_u^{(m)} = -\mathbf{q}_u + q_{u,max}$ giving $\mathbf{q}_u^{(m+1)} = q_{u,max}$. By similar reasoning we get, from block rows 10 and 11 of (S.2), $\mathbf{c}_l^{(m+1)} = 0$, and $\mathbf{c}_u^{(m+1)} = \mathbf{d}_u$. Substituting these into (S.2) gives

$$\begin{pmatrix}
\delta \mathbf{q}_b^{(m+1)} \\
\left[\mathbf{q}_{l,min}^{(m+1)} - \mathbf{q}_{l,min}^{(m)} \right] \\
\left[\mathbf{q}_{u,max}^{(m+1)} - \mathbf{q}_{u,max}^{(m)} \right] \\
\delta \mathbf{c}_b^{(m+1)} \\
\left[\mathbf{o}_{c_l}^{(m+1)} - \mathbf{o}_{c_l}^{(m)} \right] \\
\left[\mathbf{d}_{c_u}^{(m+1)} - \mathbf{d}_{c_u}^{(m)} \right] \\
\delta \mathbf{h}_{c_b}^{(m+1)} \\
\delta \mathbf{h}_{c_l}^{(m+1)} \\
\delta \mathbf{h}_{c_u}^{(m+1)} \\
\delta \boldsymbol{\lambda}^{(m+1)} \\
\delta \boldsymbol{\mu}^{(m+1)} \\
\delta \boldsymbol{\kappa}^{(m+1)} \\
\delta \boldsymbol{\nu}^{(m+1)} \\
\delta \mathbf{z}_{v_b}^{(m+1)} \\
\delta \mathbf{z}_{v_l}^{(m+1)} \\
\delta \boldsymbol{\chi}_{+0}^{(m+1)} \\
\delta \boldsymbol{\chi}_{00}^{(m+1)}
\end{pmatrix}
= -
\begin{pmatrix}
\mathbf{G}_{q_b} \mathbf{q}_b^{(m)} + \mathbf{L}_{v_b}^T \mathbf{z}_{v_b} - \mathbf{A}_b \mathbf{h}^{(m)} - \mathbf{a}_{q_b} \\
\mathbf{G}_{q_l} \mathbf{q}_l^{(m)} + \mathbf{L}_{v_l}^T \mathbf{z}_{v_l} - \mathbf{A}_l \mathbf{h}^{(m)} - \mathbf{a}_{q_l} - \boldsymbol{\kappa}^{(m)} \\
\mathbf{G}_{q_u} \mathbf{q}_u^{(m)} - \mathbf{A}_u \mathbf{h}^{(m)} - \mathbf{a}_{q_u} + \boldsymbol{\nu}^{(m)} \\
\mathbf{h}(\mathbf{c}_b^{(m)}) - \mathbf{h}_{c_b}^{(m)} \\
-\mathbf{h}_{c_l}^{(m)} + h_m + \mathbf{u}_{c_l} - \boldsymbol{\lambda}^{(m)} \\
-\mathbf{h}_{c_u}^{(m)} + h_s + \mathbf{u}_{c_u} + \boldsymbol{\mu}^{(m)} \\
-\mathbf{A}_{,b}^T \mathbf{q}^{(m)} - \mathbf{c}_b^{(m)} \\
-\mathbf{A}_{,l}^T \mathbf{q}^{(m)} - \mathbf{c}_l^{(m)} \\
-\mathbf{A}_{,u}^T \mathbf{q}^{(m)} - \mathbf{c}_u^{(m)} \\
-\mathbf{c}_l^{(m)} \\
\mathbf{c}_u^{(m)} - \mathbf{d}_u \\
-\mathbf{q}_l^{(m)} + \mathbf{q}_{l,min} \\
\mathbf{q}_u^{(m)} - \mathbf{q}_{u,max} \\
\mathbf{L}_{v_b} \left(\mathbf{S}_s \mathbf{h}^{(m)} - \mathbf{L}_{n_v} \boldsymbol{\xi}(\mathbf{q}^{(m)}) - \mathbf{z}^{(m)} + \boldsymbol{\chi}^{(m)*} - \mathbf{h}^s \right) \\
\mathbf{L}_{v_l} \left(\mathbf{S}_s \mathbf{h}^{(m)} - \mathbf{L}_{n_v} \boldsymbol{\xi}(\mathbf{q}^{(m)}) - \mathbf{z}^{(m)} + \boldsymbol{\chi}^{(m)*} - \mathbf{h}^s \right) \\
\mathbf{z}_{+0}^{(m)} \\
\mathbf{z}_{00}^{(m)}
\end{pmatrix}$$

The quantities in square brackets are zero because the index sets do not change during an iteration. As a consequence block columns 2,3,5,6 of the left-hand-side matrix can be removed and block rows 2,3,5,6 of the unknowns vector can be removed. This gives

$$\begin{pmatrix} \delta \mathbf{q}_b^{(m+1)} \\ \delta \mathbf{c}_b^{(m+1)} \\ \delta \mathbf{h}_{c_b}^{(m+1)} \\ \delta \mathbf{h}_{c_l}^{(m+1)} \\ \delta \mathbf{h}_{c_u}^{(m+1)} \\ \delta \boldsymbol{\lambda}^{(m+1)} \\ \delta \boldsymbol{\mu}^{(m+1)} \\ \delta \boldsymbol{\kappa}^{(m+1)} \\ \delta \boldsymbol{\nu}^{(m+1)} \\ \delta \mathbf{z}_{v_b}^{(m+1)} \\ \delta \mathbf{z}_{v_l}^{(m+1)} \\ \delta \boldsymbol{\chi}_{+0}^{(m+1)} \\ \delta \boldsymbol{\chi}_{00}^{(m+1)} \end{pmatrix} = - \begin{pmatrix} \mathbf{G}_{q_b} \mathbf{q}_b^{(m)} + \mathbf{L}_{v_b}^T \mathbf{z}_{v_b} - \mathbf{A}_b \mathbf{h}^{(m)} - \mathbf{a}_{q_b} \\ \mathbf{G}_{q_l} \mathbf{q}_l^{(m)} + \mathbf{L}_{v_l}^T \mathbf{z}_{v_l} - \mathbf{A}_l \mathbf{h}^{(m)} - \mathbf{a}_{q_l} - \boldsymbol{\kappa}^{(m)} \\ \mathbf{G}_{q_u} \mathbf{q}_u^{(m)} - \mathbf{A}_u \mathbf{h}^{(m)} - \mathbf{a}_{q_u} + \boldsymbol{\nu}^{(m)} \\ \hline \mathbf{h}(\mathbf{c}_b^{(m)}) - \mathbf{h}_{c_b}^{(m)} \\ -\mathbf{h}_{c_l}^{(m)} + h_m + \mathbf{u}_{c_l} - \boldsymbol{\lambda}^{(m)} \\ -\mathbf{h}_{c_u}^{(m)} + h_s + \mathbf{u}_{c_u} + \boldsymbol{\mu}^{(m)} \\ \hline -\mathbf{A}_{.b}^T \mathbf{q}^{(m)} - \mathbf{c}_b^{(m)} \\ -\mathbf{A}_{.l}^T \mathbf{q}^{(m)} - \mathbf{c}_l^{(m)} \\ -\mathbf{A}_{.u}^T \mathbf{q}^{(m)} - \mathbf{c}_u^{(m)} \\ \hline -\mathbf{c}_l^{(m)} \\ \mathbf{c}_u^{(m)} - \mathbf{d}_u \\ -\mathbf{q}_l^{(m)} + \mathbf{q}_{l,min} \\ \mathbf{q}_u^{(m)} - \mathbf{q}_{u,max} \\ \hline \mathbf{L}_{v_b} \left(\mathbf{S}_s \mathbf{h}^{(m)} - \mathbf{L}_{n_v} \boldsymbol{\xi}(\mathbf{q}^{(m)}) - \mathbf{z}^{(m)} + \boldsymbol{\chi}^{(m)*} - \mathbf{h}^s \right) \\ \mathbf{L}_{v_l} \left(\mathbf{S}_s \mathbf{h}^{(m)} - \mathbf{L}_{n_v} \boldsymbol{\xi}(\mathbf{q}^{(m)}) - \mathbf{z}^{(m)} + \boldsymbol{\chi}^{(m)*} - \mathbf{h}^s \right) \\ \hline \mathbf{z}_{+0}^{(m)} \\ \mathbf{z}_{00}^{(m)} \end{pmatrix}$$

In this system block rows 10–13 of the left-hand-side matrix are all zero and so those rows and the corresponding rows of the right-hand-side vector can be removed from the system giving

$$\begin{pmatrix}
\delta \mathbf{q}_b^{(m+1)} \\
\delta \mathbf{c}_b^{(m+1)} \\
\delta \mathbf{h}_{c_b}^{(m+1)} \\
\delta \mathbf{h}_{c_l}^{(m+1)} \\
\delta \mathbf{h}_{c_u}^{(m+1)} \\
\delta \boldsymbol{\lambda}^{(m+1)} \\
\delta \boldsymbol{\mu}^{(m+1)} \\
\delta \boldsymbol{\kappa}^{(m+1)} \\
\delta \boldsymbol{\nu}^{(m+1)} \\
\delta \mathbf{z}_{v_b}^{(m+1)} \\
\delta \mathbf{z}_{v_l}^{(m+1)} \\
\delta \boldsymbol{\chi}_{+0}^{(m+1)} \\
\delta \boldsymbol{\chi}_{00}^{(m+1)}
\end{pmatrix} = - \begin{pmatrix}
\mathbf{G}_{q_b} \mathbf{q}_b^{(m)} + \mathbf{L}_{v_b}^T \mathbf{z}_{v_b} - \mathbf{A}_b \mathbf{h}^{(m)} - \mathbf{a}_{q_b} \\
\mathbf{G}_{q_l} \mathbf{q}_l^{(m)} + \mathbf{L}_{v_l}^T \mathbf{z}_{v_l} - \mathbf{A}_l \mathbf{h}^{(m)} - \mathbf{a}_{q_l} - \boldsymbol{\kappa}^{(m)} \\
\mathbf{G}_{q_u} \mathbf{q}_u^{(m)} - \mathbf{A}_u \mathbf{h}^{(m)} - \mathbf{a}_{q_u} + \boldsymbol{\nu}^{(m)} \\
\hline
\mathbf{h}(\mathbf{c}_b^{(m)}) - \mathbf{h}_{c_b}^{(m)} \\
-\mathbf{h}_{c_l}^{(m)} + h_m + \mathbf{u}_{c_l} - \boldsymbol{\lambda}^{(m)} \\
-\mathbf{h}_{c_u}^{(m)} + h_s + \mathbf{u}_{c_u} + \boldsymbol{\mu}^{(m)} \\
\hline
-\mathbf{A}_{\cdot b}^T \mathbf{q}^{(m)} - \mathbf{c}_b^{(m)} \\
-\mathbf{A}_{\cdot l}^T \mathbf{q}^{(m)} - \mathbf{c}_l^{(m)} \\
-\mathbf{A}_{\cdot u}^T \mathbf{q}^{(m)} - \mathbf{c}_u^{(m)} \\
\hline
\mathbf{L}_{v_b} \left(\mathbf{S}_s \mathbf{h}^{(m)} - \mathbf{L}_{n_v} \boldsymbol{\xi}(\mathbf{q}^{(m)}) - \mathbf{z}^{(m)} + \boldsymbol{\chi}^{(m)*} - \mathbf{h}^s \right) \\
\mathbf{L}_{v_l} \left(\mathbf{S}_s \mathbf{h}^{(m)} - \mathbf{L}_{n_v} \boldsymbol{\xi}(\mathbf{q}^{(m)}) - \mathbf{z}^{(m)} + \boldsymbol{\chi}^{(m)*} - \mathbf{h}^s \right) \\
\hline
\mathbf{z}_{+0}^{(m)} \\
\mathbf{z}_{00}^{(m)}
\end{pmatrix}$$

Consider the subsystem made up of the block rows 1,4 and 7–15. This subsystem is independent of the unknowns $\delta \boldsymbol{\lambda}^{(m+1)}$, $\delta \boldsymbol{\mu}^{(m+1)}$, $\delta \boldsymbol{\kappa}^{(m+1)}$ and $\delta \boldsymbol{\nu}^{(m+1)}$ and so can be written

$$\begin{pmatrix}
n_{qb} & n_{cb} & n_{cl} & n_{cu} & n_{qu} & n_{vl} & n_{+0} & n_{00} \\
\mathbf{F}_{qb} & \mathbf{O} & -\mathbf{A}_{bb} & -\mathbf{A}_{bl} & -\mathbf{A}_{bu} & \mathbf{O} & \mathbf{O} & \mathbf{O} \\
\mathbf{O} & \mathbf{M}_{cb} & -\mathbf{I}_{cb} & \mathbf{O} & \mathbf{O} & \mathbf{O} & \mathbf{O} & \mathbf{O} \\
n_{cb} & -\mathbf{A}_{bb}^T & \mathbf{O} & \mathbf{O} & \mathbf{O} & \mathbf{O} & \mathbf{O} & \mathbf{O} \\
n_{cl} & -\mathbf{A}_{bl}^T & \mathbf{O} & \mathbf{O} & \mathbf{O} & \mathbf{O} & \mathbf{O} & \mathbf{O} \\
n_{cu} & -\mathbf{A}_{bu}^T & \mathbf{O} & \mathbf{O} & \mathbf{O} & \mathbf{O} & \mathbf{O} & \mathbf{O} \\
n_{vb} & -\mathbf{L}_{vb}\mathbf{F}_{qb} & \mathbf{S}_{sb} & \mathbf{O} & \mathbf{O} & -\mathbf{I}_{vb} & \mathbf{L}_{+0}^T & \mathbf{O} \\
n_{vl} & \mathbf{O} & \mathbf{O} & \mathbf{S}_{sl} & \mathbf{O} & -\mathbf{I}_{vl} & \mathbf{O} & \mathbf{L}_{00}^T \\
n_{+0} & \mathbf{O} \\
n_{00} & \mathbf{O} & \mathbf{O} & \mathbf{O} & \mathbf{O} & \mathbf{O} & \mathbf{O} & \mathbf{O}
\end{pmatrix} \times \tag{S.6}$$

$$\begin{pmatrix} \delta \mathbf{q}_b^{(m+1)} \\ \delta \mathbf{c}_b^{(m+1)} \\ \delta \mathbf{h}_{c_b}^{(m+1)} \\ \delta \mathbf{h}_{c_l}^{(m+1)} \\ \delta \mathbf{h}_{c_u}^{(m+1)} \\ \delta \boldsymbol{\lambda}^{(m+1)} \\ \delta \boldsymbol{\mu}^{(m+1)} \\ \delta \boldsymbol{\kappa}^{(m+1)} \\ \delta \boldsymbol{\nu}^{(m+1)} \\ \delta \mathbf{z}_{v_b}^{(m+1)} \\ \delta \mathbf{z}_{v_l}^{(m+1)} \\ \delta \boldsymbol{\chi}_{+0}^{(m+1)} \\ \delta \boldsymbol{\chi}_{00}^{(m+1)} \end{pmatrix} = - \begin{pmatrix} \mathbf{G}_{q_b} \mathbf{q}_b^{(m)} + \mathbf{L}_{v_b}^T \mathbf{z}_{v_b} - \mathbf{A}_b \mathbf{h}^{(m)} - \mathbf{a}_{q_b} \\ \mathbf{h}(\mathbf{c}_b^{(m)}) - \mathbf{h}_{c_b}^{(m)} \\ -\mathbf{A}_{.b}^T \mathbf{q}^{(m)} - \mathbf{c}_b^{(m)} \\ -\mathbf{A}_{.l}^T \mathbf{q}^{(m)} - \mathbf{c}_l^{(m)} \\ -\mathbf{A}_{.u}^T \mathbf{q}^{(m)} - \mathbf{c}_u^{(m)} \\ \mathbf{L}_{v_b} \left(\mathbf{S}_s \mathbf{h}^{(m)} - \mathbf{L}_{n_v} \boldsymbol{\xi}(\mathbf{q}^{(m)}) - \mathbf{z}^{(m)} + \boldsymbol{\chi}^{(m)*} - \mathbf{h}^s \right) \\ \mathbf{L}_{v_l} \left(\mathbf{S}_s \mathbf{h}^{(m)} - \mathbf{L}_{n_v} \boldsymbol{\xi}(\mathbf{q}^{(m)}) - \mathbf{z}^{(m)} + \boldsymbol{\chi}^{(m)*} - \mathbf{h}^s \right) \\ \mathbf{z}_{+0}^{(m)} \\ \mathbf{z}_{00}^{(m)} \end{pmatrix}$$

or more simply as

$$\begin{array}{c} n_{q_b} \\ n_{c_b} \\ n_{c_b} \\ n_{c_l} \\ n_{c_u} \\ n_{v_b} \\ n_{v_l} \\ n_{+0} \\ n_{00} \end{array} \begin{pmatrix} n_{q_b} & n_{c_b} & n_{c_b} & n_{c_l} & n_{c_u} & n_{v_b} & n_{v_l} & n_{+0} & n_{00} \\ \mathbf{F}_{q_b} & \mathbf{O} & -\mathbf{A}_{bb} & -\mathbf{A}_{bl} & -\mathbf{A}_{bu} & \mathbf{L}_{v_b}^T & \mathbf{O} & \mathbf{O} & \mathbf{O} \\ \mathbf{O} & \mathbf{M}_{c_b} & -\mathbf{I}_{c_b} & \mathbf{O} & \mathbf{O} & \mathbf{O} & \mathbf{O} & \mathbf{O} & \mathbf{O} \\ -\mathbf{A}_{bb}^T & -\mathbf{I}_{c_b} & \mathbf{O} \\ -\mathbf{A}_{bl}^T & \mathbf{O} \\ -\mathbf{A}_{bu}^T & \mathbf{O} \\ -\mathbf{L}_{v_b} \mathbf{F}_{q_b} & \mathbf{O} & \mathbf{S}_{s_b} & \mathbf{O} & \mathbf{O} & -\mathbf{I}_{v_b} & \mathbf{O} & \mathbf{L}_{+0}^T & \mathbf{O} \\ \mathbf{O} & \mathbf{O} & \mathbf{O} & \mathbf{S}_{s_l} & \mathbf{O} & \mathbf{O} & -\mathbf{I}_{v_l} & \mathbf{O} & \mathbf{L}_{00}^T \\ \mathbf{O} & \mathbf{O} & \mathbf{O} & \mathbf{O} & \mathbf{O} & \mathbf{L}_{+0} & \mathbf{O} & \mathbf{O} & \mathbf{O} \\ \mathbf{O} & \mathbf{O} & \mathbf{O} & \mathbf{O} & \mathbf{O} & \mathbf{O} & \mathbf{L}_{00} & \mathbf{O} & \mathbf{O} \end{pmatrix} \times \quad (\text{S.7})$$

$$\begin{pmatrix} \delta \mathbf{q}_b^{(m+1)} \\ \delta \mathbf{c}_b^{(m+1)} \\ \delta \mathbf{h}_{c_b}^{(m+1)} \\ \delta \mathbf{h}_{c_l}^{(m+1)} \\ \delta \mathbf{h}_{c_u}^{(m+1)} \\ \delta \mathbf{z}_{v_b}^{(m+1)} \\ \delta \mathbf{z}_{v_l}^{(m+1)} \\ \delta \boldsymbol{\chi}_{+0}^{(m+1)} \\ \delta \boldsymbol{\chi}_{00}^{(m+1)} \end{pmatrix} = - \begin{pmatrix} \mathbf{G}_{q_b} \mathbf{q}_b^{(m)} + \mathbf{L}_{v_b}^T \mathbf{z}_{v_b} - \mathbf{A}_b \mathbf{h}^{(m)} - \mathbf{a}_{q_b} \\ \mathbf{h}(\mathbf{c}_b^{(m)}) - \mathbf{h}_{c_b}^{(m)} \\ \hline -\mathbf{A}_{.b}^T \mathbf{q}^{(m)} - \mathbf{c}_b^{(m)} \\ -\mathbf{A}_{.l}^T \mathbf{q}^{(m)} - \mathbf{c}_l^{(m)} \\ -\mathbf{A}_{.u}^T \mathbf{q}^{(m)} - \mathbf{c}_u^{(m)} \\ \hline \mathbf{L}_{v_b} \left(\mathbf{S}_s \mathbf{h}^{(m)} - \mathbf{L}_{n_v} \boldsymbol{\xi}(\mathbf{q}^{(m)}) - \mathbf{z}^{(m)} + \boldsymbol{\chi}^{(m)*} - \mathbf{h}^s \right) \\ \mathbf{L}_{v_l} \left(\mathbf{S}_s \mathbf{h}^{(m)} - \mathbf{L}_{n_v} \boldsymbol{\xi}(\mathbf{q}^{(m)}) - \mathbf{z}^{(m)} + \boldsymbol{\chi}^{(m)*} - \mathbf{h}^s \right) \\ \hline \mathbf{z}_{+0}^{(m)} \\ \mathbf{z}_{00}^{(m)} \end{pmatrix}$$

This system can be written more compactly as (39).

PREVIOUSLY DEFINED INDEX SETS

(a)

$$\mathcal{I}_{q_b}^{(m)} = \left\{ j \in N_q \mid \left(q_j^{(m)} > q_{min,j} \wedge q_j^{(m)} < q_{max,j} \right) \vee \left(q_j^{(m)} = q_{min,j} \wedge \kappa_j^{(m)} < 0 \right) \vee \left(q_j^{(m)} = q_{max,j} \wedge \nu_j^{(m)} < 0 \right) \right\}$$

(b) $\mathcal{I}_{q_l}^{(m)} = \left\{ j \in N_q \mid \left(q_j^{(m)} < q_{min,j} \right) \vee \left(q_j^{(m)} = q_{min,j} \wedge \kappa_j^{(m)} \geq 0 \right) \right\}$

(c) $\mathcal{I}_{q_u}^{(m)} = \left\{ j \in N_q \mid \left(q_j^{(m)} > q_{max,j} \right) \vee \left(q_j^{(m)} = q_{max,j} \wedge \nu_j^{(m)} \geq 0 \right) \right\}$

(d)

$$\mathcal{I}_{c_b}^{(m)} = \left\{ i \in N_c \mid d_i > 0 \wedge \left(\left(c_i^{(m)} > 0 \wedge c_i^{(m)} < d_i \right) \vee \left(c_i^{(m)} = 0 \wedge \lambda_i^{(m)} < 0 \right) \vee \left(c_i^{(m)} = d_i \wedge \mu_i^{(m)} < 0 \right) \right) \right\}$$

(e) $\mathcal{I}_{c_l}^{(m)} = \left\{ i \in N_c \mid d_i > 0 \wedge \left(c_i^{(m)} < 0 \vee \left(c_i^{(m)} = 0 \wedge \lambda_i^{(m)} \geq 0 \right) \right) \right\}$

(f) $\mathcal{I}_{c_u}^{(m)} = \left\{ i \in N_c \mid d_i > 0 \wedge \left(c_i^{(m)} > d_i \vee \left(c_i^{(m)} = d_i \wedge \mu_i^{(m)} \geq 0 \right) \right) \right\}.$

Recall that links with no flow constraints are said formally to have upper and lower flow bounds of $\pm\infty$, while links with a PRV are said to have a lower linkflow bound of zero an upper linkflow bound of $+\infty$. The links are assigned to the index sets as follows. For each link, j :

(a) If $q_{min,j} < q_j < q_{max,j}$ then $j \rightarrow \mathcal{I}_{q_b}$

(b) If $q_j < q_{min,j}$ then $j \rightarrow \mathcal{I}_{q_l}$

(c) If $q_j > q_{max,j}$ then $j \rightarrow \mathcal{I}_{q_u}$

(d) If $q_j = q_{min,j}$ then

(i) If $\kappa_j \geq 0$ then $j \rightarrow \mathcal{I}_{q_l}$

(ii) otherwise $j \rightarrow \mathcal{I}_{q_b}$.

(e) If $q_j = q_{max,j}$ then

(i) If $\nu_j \geq 0$ then $j \rightarrow \mathcal{I}_{q_u}$

(ii) otherwise $j \rightarrow \mathcal{I}_{q_b}$.

Similarly, the outflows are assigned to their index sets as follows. For each node, i , with $d_i > 0$

(a) If $0 < c_i < d_i$ then $i \rightarrow \mathcal{I}_{c_b}$

(b) If $c_i < 0$ then $i \rightarrow \mathcal{I}_{c_l}$

(c) If $c_i > d_i$ then $i \rightarrow \mathcal{I}_{c_u}$

(d) If $c_i = 0$ then

(i) If $\lambda_i \geq 0$ then $i \rightarrow \mathcal{I}_{c_l}$

(ii) otherwise $i \rightarrow \mathcal{I}_{c_b}$.

(e) If $c_i = d_i$ then

(i) If $\mu_i \geq 0$ then $i \rightarrow \mathcal{I}_{c_u}$

(ii) otherwise $i \rightarrow \mathcal{I}_{c_b}$.

List of Tables

1	Table showing the relations between PRV status and some link and node parameters .	8
2	Network link and PRV parameters and solution values for the network shown in Fig. 7. The PRV in link 13 is active ($z_k = 40.2$ m, $q_5 = 16.8$ L/s) while the PRV in link 15 is closed ($z_{15} = 78.4$ m, $q_{15} = 0$ L/s). The flow constraint on link 14 is saturated ($q_{14} = q_{14,max} = 30$ L/s).	27
3	Network node parameters and solution values for the network shown in Fig. 7. The PRV in link 13 is active ($h_6 = 55 + 10 = 65$ m) while the PRV in link 15 is closed ($h_5 = 57.1$ m, $h_5^s = 20 + 25$ m).	28

List of Figures

1	Comparison of the functional relationship between the flow and the head loss (i) in a link with no flow or pressure control, (ii) The multivalued subdifferential mapping of an FCV device content (Rockafellar 1970) and (iii) the content of a PRV device. . . .	3
2	The network with one PRV used to generate the best reply functions shown in Fig. 3 .	8
3	The best reply functions indicating the Nash Equilibrium (●) for the network shown in Fig. 2. Flow, $q(z)$, is measured in L/s and local valve head loss, $z(q)$, is measured in m .	10
4	A model of the network used in Piller & van Zyl (2014) which has two controls, C_1 and C_2 , in series. The controls can be an FCV followed by a PRV or vice versa.	10
5	Examples of the Nash Equilibrium with two controls in series (a) FCV-PRV; the FCV constraint is saturated and the PRV is open (b) PRV-FCV; both control constraints are saturated and (c) FCV-PRV; the assumption that there is a path connecting every PRV link to a source such that no link in that path has a saturated flow constraint is violated. In all cases $q_{max} = 300$ L/s.	11
6	The local valve head loss objective function $f(z)$ for three different h^s values. For $h^s = 60$ m the PCD is fully open, for $h^s = 40$ m the PCD is active and for $h^s = 20$ m it is fully closed.	25

7	The illustrative looped network used to demonstrate a case with a saturated flow constraint, an active PRV and a closed PRV.	26
C.1	Illustration of the values of various link and node parameters for PRV: fully open state	32
C.2	Illustration of the values of various link and node parameters for PRV: active state . .	33
C.3	Illustration of the values of various link and node parameters for PRV: closed 1 state .	33
C.4	Illustration of the values of various link and node parameters for PRV: closed 2 state .	33
C.5	Illustration of the values of various link and node parameters for PRV: closed 3 state .	34